

# Interaction of particles and nuclei of high and ultrahigh energy with nuclei

V. S. Barashenkov, A. S. Il'inov, N. M. Sobolevskii, and V. D. Toneev

Joint Institute for Nuclear Research, Dubna

Usp. Fiz. Nauk 109, 91-136 (January 1973)

High energy nuclear physics has important purely scientific value and applied value. Statistical methods of calculation based on the intranuclear cascade model permit agreement to be obtained with the known experimental data over the entire energy range above several tens of MeV. For energies  $T \gtrsim 3-5$  BeV it is necessary to take into account the change in the density of intranuclear matter with development of the cascade of particles inside the target-nucleus; in the transition to the very high energy region it is necessary to take into account also many-particle interactions in which several fast particles collide with one nucleon at the same time. The methods of calculation are discussed briefly, and the results and the difficulties encountered in the calculations are considered. Special attention is devoted to interactions with targets of the light nuclei  $d$ ,  $t$ ,  $He^3$ , and  $He^4$ . Scale invariance of the interactions of high-energy particles and nuclei is discussed.

## CONTENTS

1. Introduction . . . . .	31
2. Intranuclear Cascade Mechanism . . . . .	32
3. The Nuclear Model and Calculation of Particle Collisions with Intranuclear Nucleons . . . . .	33
4. General Scheme of Cascade Calculations . . . . .	35
5. Comparison of the Cascade Model with Experiment . . . . .	37
6. Intranuclear Cascade Model in the Energy Region above Several BeV . . . . .	41
7. Intranuclear Cascades at Ultrahigh Energies $T \gg 10$ BeV . . . . .	46
8. Theory of Inelastic Collisions of Two Nuclei . . . . .	47
9. Conclusion . . . . .	49
References . . . . .	50

## 1. INTRODUCTION

High-energy nuclear physics has remained for a long time a poorly studied no man's land between elementary-particle physics and traditional low-energy nuclear physics. Many of those who have been occupied with the study of elementary particles have considered for a long time that study of the interactions of particles with such a complex system as a nucleus only complicates the picture and therefore cannot provide any information useful for elementary-particle physics. At the same time the physicists occupied with study of the nucleus itself have in turn regarded high-energy processes with great distrust, considering that the need of taking into account the complex processes associated with pion production and production of particles of other types will in essence lead them away from the problems of nuclear physics.

The situation changed radically only after it became clear that high-energy nuclear physics has important practical applications: to the calculation of radiation shielding of high flying airplanes and space ships, to the so-called electronuclear method of utilizing atomic energy and accumulating rare isotopes, to discussion of the problems of radiation stability of materials, and so forth<sup>[1-4]</sup>.

Subsequent investigations have shown convincingly that study of the phenomena occurring in collisions of high-energy particles and nuclei with nuclei is important and in many cases is the only means of obtaining information both on elementary particles and on nuclear physics. In particular, information on the interaction of particles at ultrahigh energies  $T \gtrsim 10^3$  BeV now can be obtained only from analysis of collisions of cosmic rays and nuclei with nuclei of heavy and light targets. The

details of the internal structure of nuclei also can be studied at the present time only in reactions involving particles having a very small deBroglie wavelength  $\lambda$ . The disintegration of nuclei under bombardment by intense beams of high-energy particles presents interesting possibilities for investigation of the properties of exotic nuclei far from the stability line.

Special interest in high-energy nuclear physics arose after the possibility became known of creating in the near future intense beams of relativistic nuclei in the Dubna synchrotron and other accelerators<sup>[1]</sup>. Such beams can be used for many important studies in nuclear physics and elementary-particle physics<sup>[5]</sup>. In particular, in experiments with relativistic particles we have the unique possibility of studying complex and in many respects still unexplained questions relating to the physical meaning and the possibilities of concrete description of the internal structure of relativistic objects. In contrast to elementary particles, the study of whose structure always involves relativistic effects (due, for example, to the well known problem of the time dilation of a particle<sup>[6]</sup>), we have in the case of nuclei the remarkable possibility of considering the structure of the same object both from the relativistic point of view (as is done for elementary particles) and nonrelativistically—by the methods of ordinary nuclear physics.

Although high-energy nuclear physics arose only about a quarter of a century ago, it is now one of the most rapidly developing divisions of physics. It is an extremely broad and informative field, any thorough discussion of which would require the writing of a voluminous book (such a book, "Interaction of High-Energy Particles and Nuclei with Nuclei" by V. S.

Barashenkov and V. D. Toneev, was published by The Atomic Publishing House in 1972). The purpose of the present review is to draw the attention of a wide group of readers to this interesting and very promising field of physics, to discuss the main features of the very complex phenomena occurring here, and to present the current state of the theory, emphasizing those aspects which are still unclear and require further investigation<sup>2)</sup>.

In what follows we will designate as high-energy all particles and nuclei with a wavelength  $\lambda$  several times less than the dimensions of the target-nucleus. For nucleons and mesons this corresponds to the energy region T above several tens of MeV<sup>3)</sup>.

We limit the discussion to inelastic nuclear interactions. A number of thorough books and reviews exist in the field of elastic interactions (see, for example, refs. 7-10, where a further bibliography can be found).

## 2. THE INTRANUCLEAR CASCADE MECHANISM

The inelastic collision of a high-energy particle with a nucleus, and even more the collision of two nuclei, is a very complex and multifaceted phenomenon whose analytical description encounters considerable difficulties. In recent years all calculations of such collisions have been carried out, as a rule, by statistical modeling by the Monte Carlo method.

This approach was apparently first developed by Goldberger<sup>[11]</sup>, who in turn based his work on the idea of Heisenberg and Serber, who regarded intranuclear cascades as a series of successive quasifree collisions of the fast primary particle with the individual nucleons of the nucleus.

In the two decades which have passed since the publication of Goldberger's work, the application of the Monte Carlo method to calculation of intranuclear cascades has been studied by many authors; during this time the technique of the calculations was substantially improved, more accurate nuclear models began to be used, and the information on intranuclear  $\pi N$  and  $NN$  interactions expanded and improved. However, most work considered only interactions at energies  $T < 0.5-0.7$  BeV, where it was possible to neglect pion-production processes, as a result of which the calculations were substantially simplified.

The production of mesons was taken into account for the first time in the well known work of Metropolis and co-workers<sup>[12]</sup> and in work performed at Dubna<sup>[13-17]</sup>. Significant progress in this respect was made by Bertini<sup>[18]</sup>. Major difficulties were involved also with the simultaneous inclusion in Monte Carlo calculations of the conservation of energy and momentum; only recently has it become possible to cope satisfactorily with this difficulty<sup>[14, 19]</sup>.

Special attention is deserved by the very high energy region  $T \gg 10$  BeV, where it is necessary to take into account processes in which an intranuclear nucleon simultaneously absorbs several high-energy mesons (so called many particle interactions)<sup>[16, 17]</sup>.

It is easy to see that the main condition for applicability of the intranuclear cascade model is that the DeBroglie wavelength  $\lambda$  of the particles participating in the interaction be sufficiently small: it is necessary that for most of these particles  $\lambda$  be less than the aver-

age distance between the intranuclear nucleons  $\Delta \sim 10^{-13}$  cm. Only in this case does the picture acquire quasiclassical features and can we speak approximately of particle trajectories and two-particle collisions inside the nucleus. It is clear that for this to be the case the primary particle energy T must be greater than several tens of MeV.

Another important condition for applicability of the intranuclear cascade model is the requirement that the time in which an individual two-particle intranuclear collision occurs on the average,  $\tau \sim 10^{-23}$  sec, be less than the time interval between two such consecutive interactions

$$\Delta t = l/c \gg 4\pi R^2/3A\sigma \gg 3 \cdot 10^{-22}/\sigma \text{ (mb) sec,}$$

where  $l$  is the mean range of the cascade particle before the interaction,  $c$  is the velocity of light,  $R = r_0 A^{1/3}$  is the mean radius of the nucleus, and  $\sigma$  is the cross section for interaction with an intranuclear nucleon. This permits the interaction of the incident particle with the nucleus to be reduced to a set of individual statistically independent intranuclear collisions.

The requirement  $\tau < \Delta t$  is equivalent to the requirement that the intranuclear interaction cross section be sufficiently small:  $\sigma \lesssim 100 \xi$ , where the coefficient  $\xi \sim 1$ .

Since the energy of the particles participating in the cascade is rather large—as a rule significantly greater than the binding energy of the intranuclear nucleons—the same characteristics can be used for interaction of cascade particles inside the nucleus as for the interaction of free particles. The effect of other intranuclear nucleons is taken into account by introduction of some averaged potential  $V$ , and also by the action of the Pauli principle<sup>4)</sup>.

We can say that a high-energy particle which has entered the nucleus passes through a gas of free nucleons, producing a cascade (avalanche) of secondary particles. A fraction of these secondary particles leaves the nucleus, and the remaining fraction is absorbed, exciting the nucleus to some energy  $E^*$ .

In Fig. 1 we have shown an example of the history of a proton with energy 660 MeV inside a  $Ru^{100}$  nucleus (we will discuss the details of the calculation of such histories in more detail below). As can be seen from

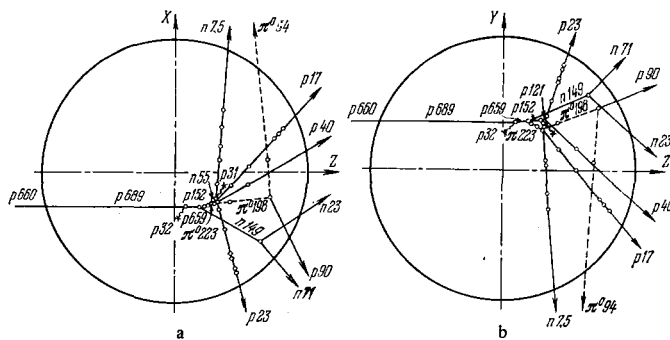


FIG. 1. Intranuclear cascade initiated in  $Ru^{100}$  by a 660-MeV proton. a) Projection on the X, Z plane; b) projection on the Y, Z plane. The numbers with the particle symbols are their kinetic energy in MeV. The circles in the particle trajectories are the points of collisions which could occur but were forbidden by the Pauli principle. The wavy lines indicate trajectories of recoil nucleons which stopped inside the nucleus, and the dashed lines are  $\pi$ -meson trajectories.

the figure, the primary proton, entering the nucleus and increasing its energy by an amount equal to the depth of the potential well, is elastically scattered by an intranuclear proton. The recoil proton with energy  $\mathcal{E} = 32$  MeV is lost in the nucleus since its kinetic energy  $\mathcal{E} \approx V_p$ , where  $V_p \approx 31$  MeV is the depth of the potential well for a proton in the  $\text{Ru}^{100}$  nucleus. After the elastic scattering the primary proton, having changed its direction somewhat and having lost an energy  $\Delta\mathcal{E} \approx 30$  MeV, again collides, this time inelastically, with an intranuclear neutron, creating a  $\pi^0$  meson with energy  $\mathcal{E} = 223$  MeV. The neutron undergoes an additional collision inside the nucleus, after which both secondary particles (neutrons) leave the nucleus with energies of 23 and 71 MeV (after subtraction of the potential energy  $V \approx 35$  MeV). The proton in turn is further scattered elastically, first by a neutron, and then by a proton, which leads to emission from the nucleus of two protons and a neutron with respective energies of 23, 40, and 7.5 MeV.

We note that the neutron also undergoes one elastic scattering in the nucleus; however, the recoil-proton energy ( $\mathcal{E} \approx 31$  MeV) turns out to be insufficient for this proton to leave the nucleus. The  $\pi^0$  meson produced is successively scattered by two intranuclear protons and leaves the nucleus, having an energy of 94 MeV (after subtraction of the potential energy  $V_\pi \approx 25$  MeV). The recoil protons also leave the nucleus.

It can be seen from Fig. 1 that there could be many more intranuclear collisions if a substantial part of them (especially for low-energy particles) were not forbidden by the Pauli principle. It is important to emphasize that the example discussed is an individual single event and does not answer the question of what are the characteristics of the proton-nuclear interaction at  $T = 660$  MeV. In order to answer this question, it is necessary to consider a rather large number of individual histories not related to each other. However, the main factors involved in the calculation of inelastic interactions of particles with nuclei are already evident in this example.

After the interaction shown in Fig. 1, the nucleus is left with an excitation energy of about 105 MeV (this follows directly from the reaction energy balance). Statistical equilibrium, as a rule, is established between the nucleons of this nucleus, and the subsequent transition to lower excited states occurs by successive (and sometimes also multiple) emission of nucleons and the light nuclei  $d$ ,  $t$ ,  $\text{He}^3$ , and  $\text{He}^4$ . The transition to the ground state occurs by emission of  $\gamma$  rays.

In light nuclei, where the excitation energy is quite large compared to the total binding energy, instead of the successive emission of particles, the preferred process turns out to be the direct decay of the nucleus to nucleons and heavier fragments, such as occurs, for example, in the theory of multiple production of Fermi particles in decay of the compound system formed as the result of collision of two high-energy particles.

It is important to note that while the cascade (fast) stage of the interaction occurs in a time of the order  $10^{-22}$ – $10^{-23}$  sec, the decay of the excited residual nucleus (the slow stage) is characterized by substantially longer times. At the same time, in addition to equilibrium nuclear-decay processes, comparatively fast nonequilibrium phenomena also occur in which the

nucleus cools off by emission of one or two particles, after which equilibrium is established and the stationary decay processes mentioned above occur.

The contribution of nonequilibrium processes increases with increasing excitation energy  $E^*$  and becomes very important at high incident-particle energies  $T$ . Calculation of the decay of the excited nuclei is carried out today, as a rule, also by the Monte-Carlo method (the so-called evaporative cascade). We see that calculation of the inelastic interaction of a high-energy particle is a complex physical and mathematical problem.

### 3. THE NUCLEAR MODEL AND THE CALCULATION OF COLLISIONS OF PARTICLES WITH INTRANUCLEAR NUCLEONS

Before calculating intranuclear cascades, we must store in the computer memory a description of the nuclear structure and the properties of elastic and inelastic  $\pi N$  and  $NN$  interactions inside the nucleus (their cross sections and the characteristics of the secondary particles).

Since we are dealing with the region of rather high energies where the energies of the cascade particles as a rule are significantly greater than the binding energy of the intranuclear nucleons, the details of the structure of the target-nucleus have a comparatively small effect on the results of the calculations. Within the accuracy of current experimental data it turns out to be quite sufficient to consider the nucleus as a degenerate Fermi gas of protons and neutrons enclosed in a spherical well with a diffuse boundary. The parameters of this well are determined from comparison of theoretical results with experiment and turn out to be extremely close to the values which follow from experiments on scattering of high-energy electrons (the differences can be assigned mainly to the effect of the finite size of the primary particle).

The effect of the nuclear nucleons on the particle hitting a nucleus can be taken into account by adding to its kinetic energy some averaged potential  $V(r)$ . The spatial distribution of this potential is usually chosen the same as the distribution of the density of intranuclear nucleons.

With the exception of the recent results of the Brookhaven group (G. Friedlander, K. Chen, J. H. Miller, et al.), none of the studies carried out up to the present time have taken into account the dependence of the nuclear potential on the energy of the fast particle, although the analysis of experimental data by means of the optical model indicates that such a dependence exists. In essence the potential  $V$  is at the present time a parameter of the theory, although in the case of nucleons some theoretical estimates of this quantity can be obtained.

One of the most serious difficulties arising in calculation of intranuclear cascades lies in the necessity of having available in the computer detailed information on the inelastic interactions of particles at various energies. This not only imposes severe requirements on the size of the core memory, but in many cases—particularly in the energy region where multiple production of particles is important—turns out to be generally impossible because of the absence of the necessary experimental data.

At the present time two different approaches are known which permit this difficulty to be at least partially avoided. In the first approach some theoretical model is used to describe the inelastic interaction of the particles (for example, the assumption that all pion production occurs as the result of decay of  $\pi N$  resonances  $N_{33}^*(1236)$ ,<sup>[18]</sup> or various versions of the peripheral and multiperipheral models<sup>[20]</sup>). However, since we do not have available a theory of strong interactions, all of these models are crude and, what is more important, extremely limited approximations and furthermore often require extended numerical calculations (particularly when the peripheral and multiperipheral models are used<sup>5)</sup>).

At the same time we wish to caution readers about use of the so-called random stars from the work of Kopylov<sup>[21]</sup>. The angular distributions of the particles in these stars have nothing in common with experiment. This is due to the fact that the calculation of these stars was based on the Fermi model, which in fact cannot be used to describe angular distributions.

Grave doubts are raised also by all subsequent work devoted to composition of an atlas of random stars by calculation of known analytical expressions. In essence, instead of having a standard program for calculation of values of some analytical expression and accurately calculating these values for given parameters each time when this is required, in this approach it is proposed to store a large quantity of calculated values and obtain approximate values by subsequent statistical analysis of the stored values.

The second approach is based on use of average experimental distributions (angular, momentum, and so forth) from which by the Monte-Carlo method selections are made which permit the result of an individual inelastic-interaction event to be reproduced.

As detailed calculations carried out over a number of years at Dubna have shown, this approach is quite effective and can be successfully used in computers with even a relatively small core memory (4000 to 8000 words).

Instead of the differential distributions  $w_\theta(\cos \theta)$  and  $w_p(p)$ , it is more convenient for this purpose to take as a basis the corresponding integral equations

$$W_\theta(\cos \theta) = \int_0^{\cos \theta} w_\theta(2z-1) dz \left( \int_0^1 w_\theta(2z-1) dz \right)^{-1},$$

$$W_p(p) = \int_0^p w_p(zp_{\max}) dz \left( \int_0^1 w_p(zp_{\max}) dz \right)^{-1},$$

which are smoother functions of angle and momentum.

In a Monte-Carlo calculation the values of angle and momentum are determined for each particle as inverse

functions  $\cos \theta = W_\theta^{-1}(\xi)$  and  $p = W_p^{-1}(\xi)$  of a random number  $\xi$  uniformly distributed in the interval  $[0, 1]$ . When conservation of energy is taken into account, this automatically gives the average secondary-particle multiplicity  $\bar{n}$ .

It must be emphasized that this approach can in no way be considered as a theory of the inelastic interaction of two particles; this is only the phenomenological description of the individual interaction characteristics important in this case. The suitability of such a description is justified only by comparison with experiment.

Use of additional conditions in the form of rejection of selections in accordance with the experimental distributions of various new characteristics (for example, the requirement that the selections of quantities obtained by random choice of angular and energy distributions be consistent with the experimental distribution of transverse momentum) permits the limits of reproducible characteristics to be extended considerably. Of course, in this case the calculation time increases, since the calculation of the rejected events must be carried out again.

The calculations are still further simplified if for  $W_\theta^{-1}(\xi)$  and  $W_p^{-1}(\xi)$  we use the polynomial approximations

$$\cos \theta = 2\xi^{1/2} \left[ \sum_{n=0}^N a_n \xi^n + \left(1 - \sum_{n=0}^N a_n\right) \xi^{N+1} \right] - 1,$$

$$p = p_{\max} \xi^{1/2} \left[ \sum_{n=0}^N b_n \xi^n + \left(1 - \sum_{n=0}^N b_n\right) \xi^{N+1} \right],$$

where  $p_{\max}$  is the largest observed momentum value in the experimental spectrum,

$$a_n = \sum_{k=0}^M a_{nk} T^k, \quad b_n = \sum_{k=0}^M b_{nk} T^k, \quad p_{\max} = \sum_{k=0}^M c_k T^k.$$

The coefficients  $a_{nk}$ ,  $b_{nk}$ , and  $c_k$  can be considered as constants for wide intervals  $\Delta T$ .

The finding of such approximations involves extremely laborious numerical analysis of a large amount of experimental data; however, after this has been carried out, the approximations obtained can be used for calculation of cascades in various nuclei and for various energies. The details of the calculations and tables of the coefficients approximating the experimental angular and energy distributions of the particles produced for the range of energies from several tens of MeV to  $T \sim 10^3$  BeV can be found in refs. 19 and 20<sup>6)</sup>.

Examples of agreement of the theoretical and experimental values are shown in Table I and in Figs. 2-5. It is interesting to note that we can describe satisfactorily in this way not only inelastic interactions but also the angular distributions of elastically scattered particles (Fig. 6).

TABLE I. Distribution of inelastic pp interactions in number of charged particles produced  $n_\pm$  (in %)

T, MeV		$n_\pm$					
		2	4	6	8	10	12
2	Theory	88.4±3.0	11.6±1.1				
	Experiment <sup>23</sup>	88.9±1.7	11.1±0.6				
9	Theory	32.0±1.8	47.8±2.2	18.6±1.4	1.6±0.4		
	Experiment <sup>24</sup>	44.8±4.2	42.2±4.1	10.6±2.1	2.4±0.6		
14	Theory	25.6±1.6	50.8±2.3	21.2±1.4	2.4±0.5	0	
	Experiment <sup>25</sup>	33.3±4.6	42.8±5.2	20.8±3.6	2.5±1.3	0.6±0.6	
27	Theory	14.4±1.2	35.2±1.9	33.6±1.8	14.0±1.2	2.8±0.5	0
	Experiment <sup>26</sup>	19.8±2.9	33.9±3.4	28.1±3.2	13.0±2.4	4.0±2.4	1.0±0.7

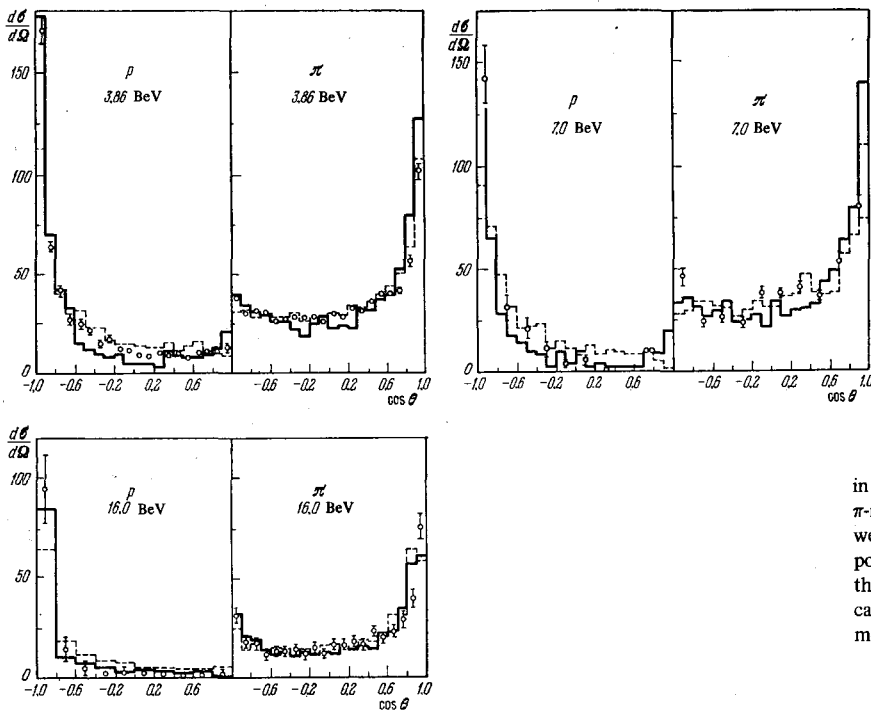


FIG. 2. Angular distributions of particles produced in reactions  $\pi^- + p \rightarrow N + n\pi$  ( $n > 2$ ). The primary  $\pi$ -meson energy is shown in the figure. The histograms were calculated by the Monte-Carlo method with polynomial approximations. The dashed lines show the distributions calculated without additional discarding of events on the basis of the transverse momentum  $p_1$  (CMS).

There is an additional circumstance which substantially affects the accuracy of the cascade calculations—the necessity of observing accurately the conservation of energy and momentum in the Monte-Carlo reproduction of each inelastic  $\pi N$  or  $NN$  interaction. For calculation of integrated average quantities such as the average multiplicity and the average secondary-particle energy, it is sufficient to take into account these laws statistically in the average over a large number of interactions<sup>[16,17,20,31]</sup>. Satisfactory results are obtained in this way also for the total angular and energy distributions.

In Fig. 7 we have shown for various types and energies of incident particles the distribution of the difference in the total energies of the system of particles before and after the interaction. The average value  $\epsilon_1$  the energy difference is actually hardly different from zero, but the dispersion turns out to be unexpectedly large and the tail of the distribution extends up to values  $\Delta E \approx T$ . This can lead to quite substantial errors in such characteristics as the number of particles in a certain energy interval, the spectrum of particles at a certain angle, and so forth; the excitation energy of the residual nucleus and, consequently, the number of black prongs in the star turn out to be particularly sensitive<sup>[32]</sup>.

In order to avoid this difficulty, a special method was developed in our laboratory for Monte Carlo simulation of inelastic interactions of elementary particles with accurate inclusion of the conservation of energy and momentum in each individual interaction event (this is reported in more detail elsewhere<sup>[19]</sup>).

#### 4. GENERAL SCHEME OF CASCADE CALCULATIONS

After the choice of a nuclear model and an algorithm for determination of the  $\pi N$  and  $NN$  interaction characteristics (for this purpose it is necessary to store in the computer memory also the values of the integrated cross sections for elastic and inelastic interactions

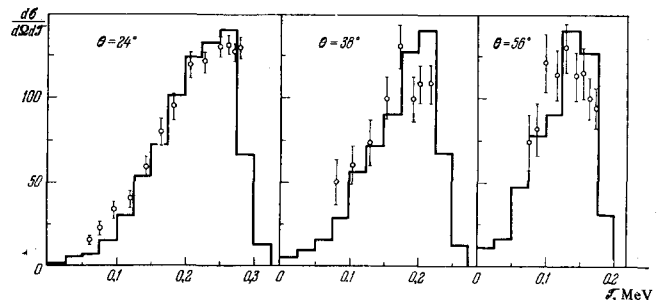


FIG. 3. Energy spectra of charged mesons at angle  $\theta$  in the reaction  $p + p \rightarrow 2N + \pi$  at  $T = 670$  MeV. Histograms—result of Monte Carlo calculation (laboratory system).

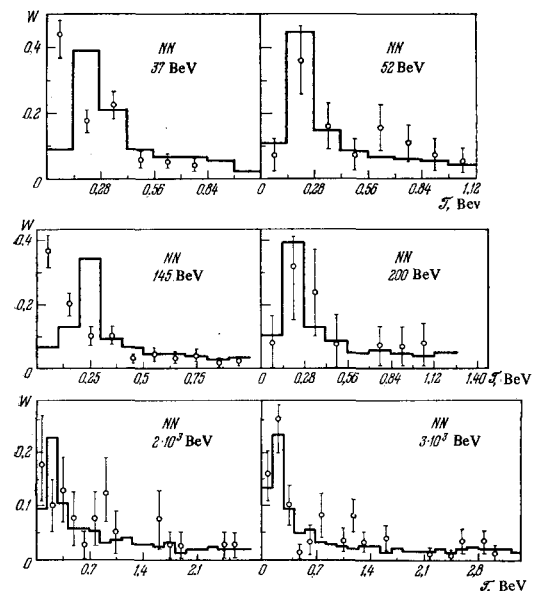


FIG. 4. Distribution of kinetic energies of secondary particles in inelastic  $NN$  collisions for various average energies  $T$ . Center-of-mass system, histograms—theory; the experimental points were taken from refs. 27–29.

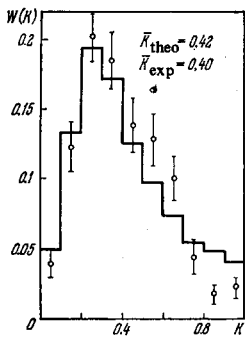


FIG. 5. Distribution of inelasticity coefficient in NN collisions at  $T > 10$  BeV. Histogram—theory, points—average experimental data for the interval  $T = 2-5 \times 10^4$  BeV from Refs. 27, 28, 30. Average values of  $\bar{K}$  are given ( $\bar{K}_{\text{exp}}$  for  $T = 200-400$  BeV) (CMS).

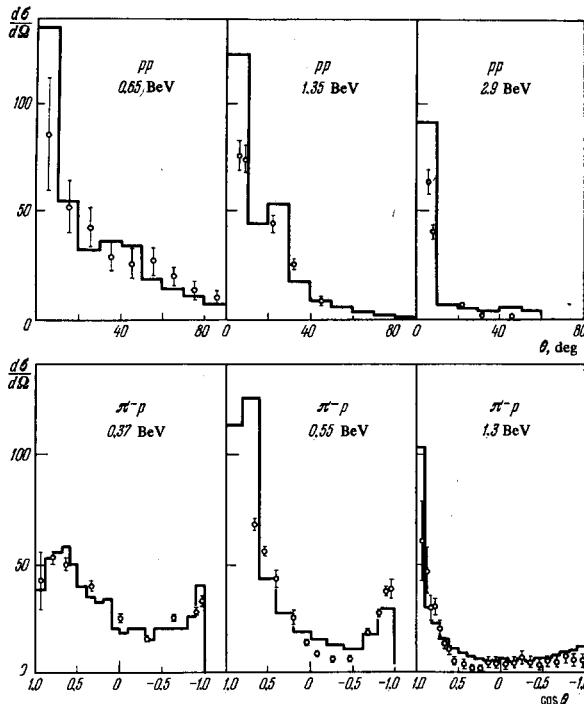


FIG. 6. Angular distributions of elastically scattered particles. Histogram—result of Monte Carlo calculation with polynomial approximation (CMS).

$\sigma_{el}(T)$  and  $\sigma_{in}(T)$ , calculation of the intranuclear cascade is carried out according to the scheme shown in Fig. 8. The rectangular boxes in the diagram denote operations which are definite logically closed parts of the program. The oval boxes denote logical operations which control the various branchings of the program (transfer conditions).

Box 1 takes into account the change in primary-particle momentum due to the effect of the intranuclear potential and to refraction and reflection of the DeBroglie wave of the particle at the nuclear boundary.

In the next box 2 are chosen the momentum and isospin (proton or neutron) of the intranuclear nucleon with which the interaction occurs (for brevity we will call this nucleon the partner), and from the given elementary cross section  $\sigma_t(t) = \sigma_{el}(t) + \sigma_{in}(t)$  (where  $t$  is the relative energy of the primary particle and the partner taking part in the intranuclear motion) the mean free path of the particle in nuclear matter  $L = L(\sigma_t)$  is calculated and the point of interaction is determined.

Box 3 tests whether this point of interaction is inside the nucleus. If it is not, then the particle is assumed to have passed through the nucleus without interaction.

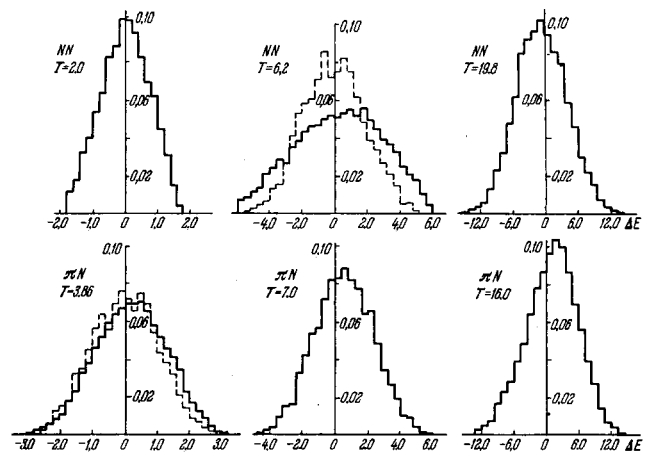


FIG. 7. Distribution of energy difference  $\Delta E$  (BeV, laboratory system) in NN and  $\pi N$  interactions at energy  $T$ , BeV. The dashed lines show the distributions calculated with the simplifying assumption of isotropic emission of the particles produced.

The ratio of the number of such particles to the total number of interactions considered with the nucleus  $N_t$  obviously characterizes the reaction cross section  $\sigma_{in}$ .

If the point of interaction is inside the nucleus, then the type of interaction: elastic or inelastic, is determined from the known cross sections  $\sigma_{el}(t)$  and  $\sigma_{in}(t)$  in the box 4.

In box 5 the secondary-particle characteristics are determined in accordance with the type of interaction selected (the nature, number, energy, and the emission angle).

Box 6 is a test of whether the Pauli principle is satisfied. Interactions which do not satisfy this principle are considered forbidden and the particle trajectory is followed beyond the point of the forbidden interaction (in Fig. 1 these forbidden interaction points in the particle trajectories are marked by circles; there are a good many of these points).

In the next box 7 the particle energy  $\mathcal{E}$  is compared with some previously specified cutoff energy  $\mathcal{E}_{\text{cut}}$  which determines whether this particle is sufficiently energetic ( $\mathcal{E} > \mathcal{E}_{\text{cut}}$ ) to take further part in development of the intranuclear cascade or whether its energy is so small ( $\mathcal{E} \leq \mathcal{E}_{\text{cut}}$ ) that the particle is simply absorbed by the nucleus. In the first case the particle is followed further as was described above. (For this the parameters of all cascade particles with energy  $\mathcal{E} > \mathcal{E}_{\text{cut}}$  are stored in the memory in box 8 and later the cascade calculation is repeated for each of them in turn by going to boxes 9 and 2.) In the second case the treatment of this particle is terminated; in box 10 this particle contributes to the excitation energy of the residual nucleus.

The calculation is carried out until all particles are absorbed or leave the nucleus. The operations in boxes 8, 9 and 11 are responsible for this. If the history of the one particle which entered the nucleus has been completed (i.e., if the computer memory is empty; see box 11), the history of the next particle is then simulated (boxes 12 and 13), and so forth.

Box 10 accumulates and processes the resulting information, including storage on magnetic tape, composition and printing of histograms of the required type,

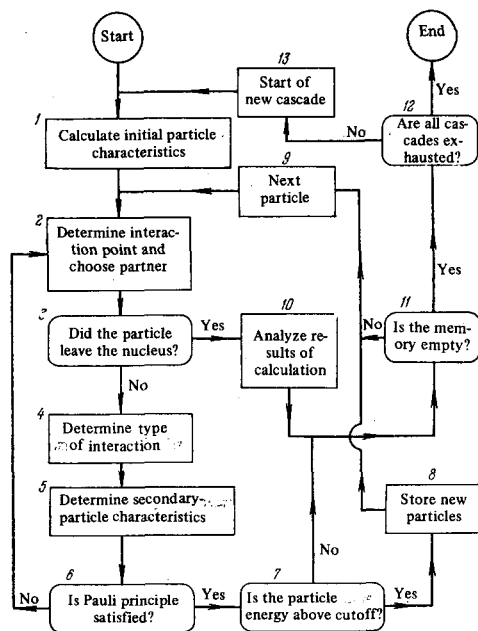


FIG. 8. General diagram of the intranuclear cascade calculation.

calculation of averages, evaluation of statistical errors of the calculation, and so forth.

Any cascade calculation at not very high energies where it is still possible to neglect many-particle interactions and the change in density of the intranuclear nucleons (more about this later) can be fitted into the general scheme shown in Fig. 8. The specific form of the box operations and their complexity are determined by the choice of the nuclear model and by the number and variety of elementary processes which it is considered necessary to take into account in a given calculation. The individual boxes can be studied in more detail in ref. 19.

In regard to the decay of the excited residual nucleus, we will not discuss this part of the program at present, since this would take us far into the field of low-energy nuclear physics. We refer those who are interested in this subject to the reports and articles listed in refs. 33-55, where a further bibliography can be found.

## 5. COMPARISON OF CASCADE MODEL WITH EXPERIMENT

Comparison of the intranuclear cascade model with experiment has been carried out by many workers (see in particular refs. 2, 12, 36, and 37, where a bibliography is given). However, this comparison has been limited principally to the relatively low-energy region where meson-production processes can be neglected.

At higher energies for the most part only the average characteristics of interactions have been compared with experiment, and only in individual cases have the differential angular and momentum distributions been discussed. Such a comparison permits us to obtain a correct general representation of the nature of the interaction of a particle with a nucleus, but some important details can be missed, especially since the calculations made by different authors refer to different energy regions, and the use for description of  $\pi N$  and  $NN$  interactions inside the nucleus of experimental data averaged over an energy interval which is wide and

which varies from study to study can mask anomalies in behavior of the theoretical quantities.

An additional source of inaccuracy in the calculations is the use of a crude nuclear model which does not take into account the diffuseness of the boundary, neglect of the potential acting on mesons inside the nucleus, and neglect of energy and momentum conservation.

Except for the very high cosmic-ray energy region where experiments are very difficult and the region  $T \lesssim 200$  MeV where the calculations are simplified as a result of the fact that it is not necessary to take into account pion production, the accuracy of all cascade calculations made up to the present time has been appreciably lower than the experimental accuracy. Rather accurate calculations in the energy region up to several BeV and above have been made only very recently<sup>[14, 15, 18, 35, 38, 39]</sup>. The degree of agreement between the theoretical and experimental values can be seen from Figs. 9-16 and Tables II and III.

If we limit ourselves to the energy region not exceeding several BeV (higher energies will be discussed below), significant deviations occur only at energies  $T \approx 50-100$  MeV and where doubly differential distributions are involved; the differences are already not so noticeable in the integrated quantities<sup>[48]</sup>. (We recall that at energies of the order of several tens of MeV the de Broglie wavelengths of the cascade particles become already comparable with the dimensions of the target-nucleus; in this case a more rigorous inclusion of quantum effects is necessary.)

A certain disagreement of the theoretical and experimental distributions of  $d^2\sigma/d\Omega dT$  is observed also in the region of the quasielastic-scattering peak<sup>[39]</sup>. However, these disagreements are not very critical and apparently can be removed by a more careful selection of

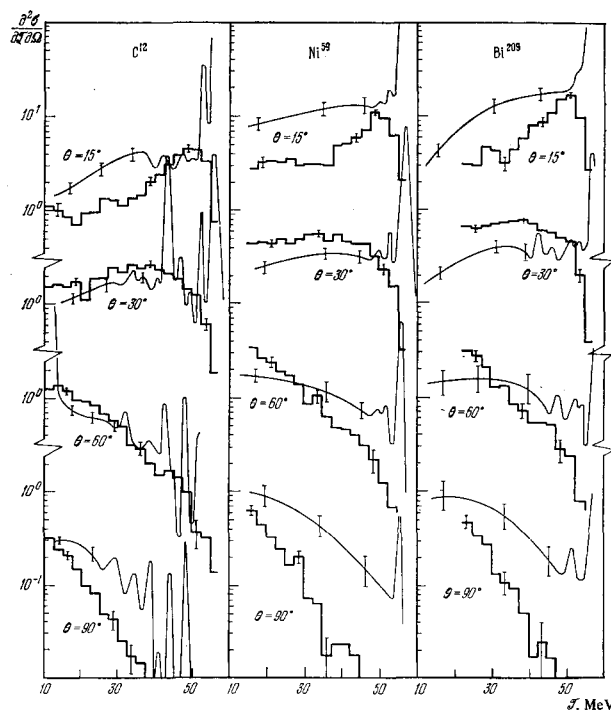


FIG. 9. Energy spectra of protons emitted at angle  $\theta$  from various nuclei bombarded in a proton beam with energy  $T = 57$  MeV (in units of  $\text{mb}/\text{MeV}\cdot\text{sr}$ ). Histograms—theory; the experimental curves were taken from ref. 40.

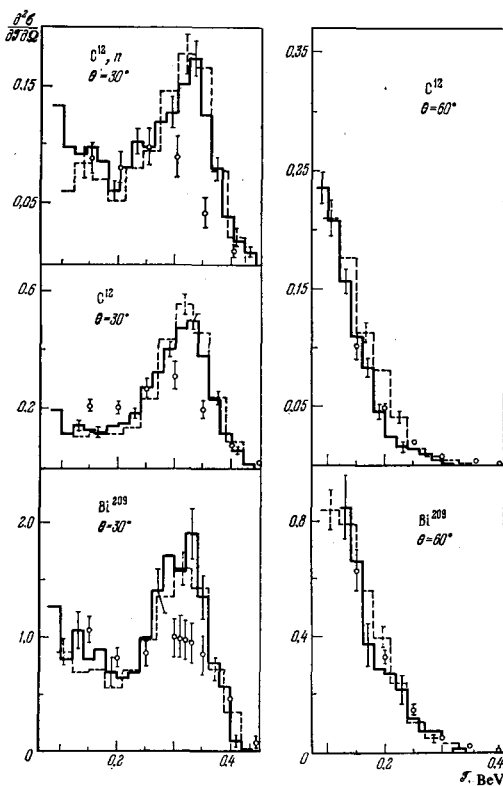


FIG. 10. Energy spectra of protons and neutrons (upper left figure) emitted from carbon and bismuth nuclei bombarded by primary protons with energy  $T = 450$  MeV (in units of  $\text{mb}/\text{MeV}\cdot\text{sr}$ ). Solid histograms—our calculation dashed histograms—calculation of Bertini [18]; the experimental points were taken from ref. 41.

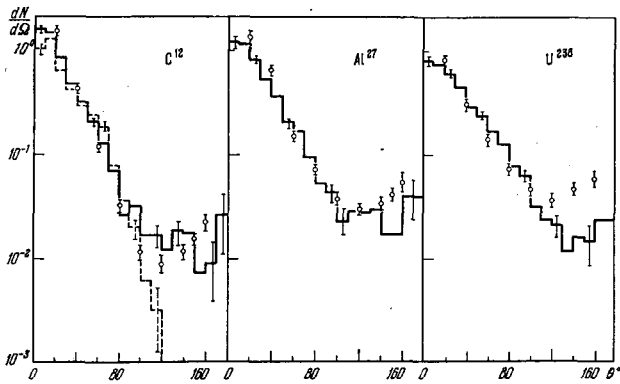


FIG. 11. Angular distributions of nucleons with energy  $E > 60$  MeV produced in interactions of 660-MeV protons with various nuclei (in units of  $\text{nucleons}/\text{MeV}\cdot\text{sr}\cdot\text{proton}$ ). Histograms—theory; the dashed line for  $\text{C}^{12}$  shows the results of calculations not taking into account pion-production processes; the experimental points were taken from ref. 42.

the model parameters and more careful approximation of the NN interaction events inside the nucleus.

The same can also be said of other differences between theory and experiment which have been noted in some studies at  $T \approx 1$  BeV. As a rule, these discrepancies turn out to be due not to breakdown of the cascade mechanism but to imperfection in the specific cascade-theory version used [35, 36].

In addition, for a comparison it is very important to take into account the specific experiment, as can easily be seen, for example, from Fig. 15. In the work of Berkovitch et al. [45] the information on the average

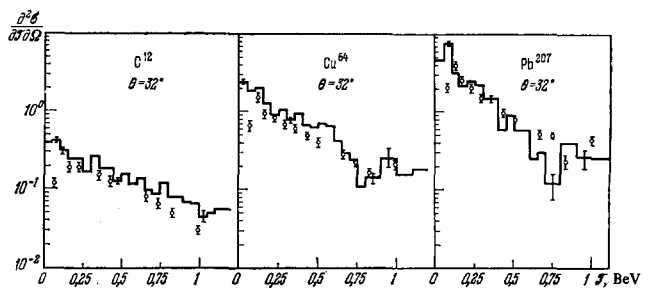


FIG. 12. Energy spectra of protons emitted from various nuclei bombarded by primary protons with energy  $T = 3$  BeV (in units of  $\text{mb}/\text{MeV}\cdot\text{sr}$ ). Histogram—theory; the experimental points were taken from ref. 43.

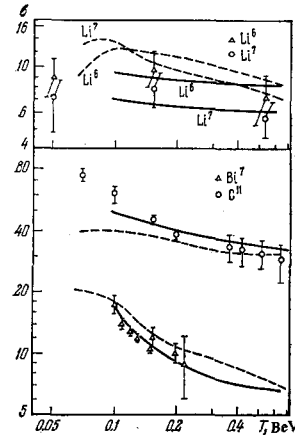


FIG. 13

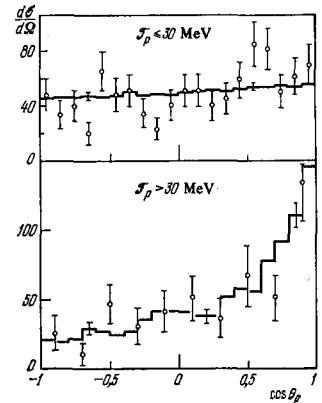


FIG. 14

FIG. 13. Energy dependence of cross sections for production of various isotopes in the reactions  $p + \text{C}^{12}$  (in  $\text{mb}$ ). Curves—theoretical results. The dashed lines show data obtained without taking into account diffuseness of the nuclear boundary and pion-production processes. A bibliography of the articles from which the experimental points were taken is given in ref. 34.

FIG. 14. Comparison with theory of experimental angular distributions of protons from stars with a number of prongs  $n \geq 2$  produced in photoemulsion by bremsstrahlung photons with energy  $T \leq T_{\text{max}} = 1150$  MeV (in arbitrary units). Histograms—theory; the experimental points were taken from ref. 44.

number of low-energy neutrons  $\bar{n}_n$  was obtained from cosmic-ray experiments in which thick targets were used, which results in somewhat exaggerated values of  $\bar{n}_n$ . In the work of Vasil'kov et al. [46] all neutrons emitted at angles  $\theta > 30^\circ$  were designated low-energy; it is understandable that a significant fraction of the cascade particles were also recorded in this region in addition to the evaporation particles. Inclusion of the contribution of these particles substantially improves the agreement of theory and experiment.

In the energy region  $T \lesssim 300$  MeV where pion production is not important, the results of our calculations [35, 36] are close to the values given by Bertini [36]. However, there are appreciable differences in the pion yield, especially for  $T \approx 300$  MeV. It is possible that this is a manifestation of the somewhat different choice of meson-nuclear potential  $V_\pi$  made by us and by Bertini and, for  $T \approx 300$  MeV, also the fact Bertini did not take into account meson-production processes. (It should be noted that in reconciling the theoretical values for  $\pi$  mesons with experiment it turns out to be very important to take into account the potential  $V_\pi \approx 25$  MeV and the absorption of  $\pi$  mesons by pairs of intranuclear nucleons [14]).

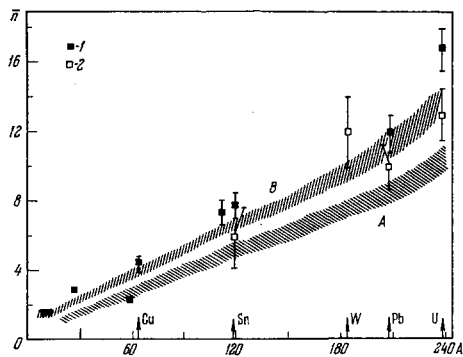


FIG. 15. Average number of low-energy neutrons as a function of target-nucleus mass number. The primary-proton energy is  $T = 660$  MeV. The shaded regions indicate the uncertainty in the calculation: A—for neutrons with energy  $\mathcal{E} < 30$  MeV, B—for that part of the neutrons which are emitted at angles  $\theta \geq 30^\circ$ . The symbols marked 1 and 2 show the experimental points from refs. 45 and 46.

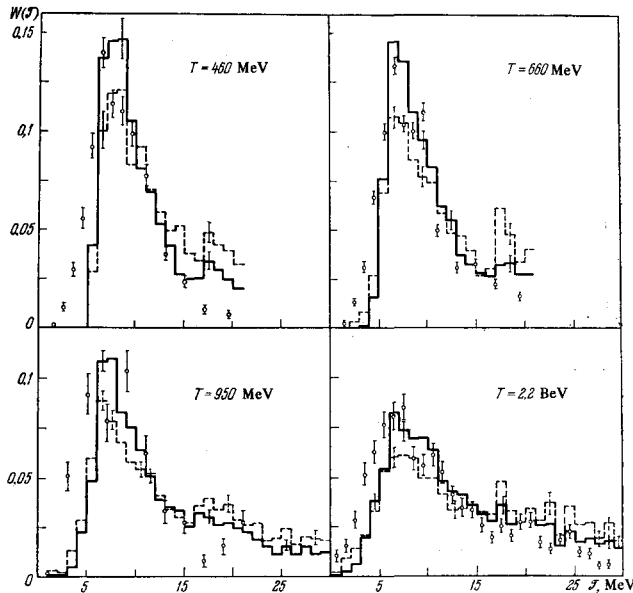


FIG. 16. Energy spectra of protons evaporated from heavy photoemulsion nuclei bombarded by protons of energy  $T$  (in relative units). Solid and dashed histograms—calculation for level density parameters  $a = A/10$  and  $A/20$ , respectively. A bibliography of the articles from which the experimental points have been taken is given in ref. 35.

Comparison with the published results of the calculations at higher energies (see refs. 2, 12, and 49) reveals a difference in a number of details. An analysis has shown that the disagreements of the calculations made at Dubna<sup>[35, 36]</sup> and the data of Metropolis et al.<sup>[12]</sup>, for example, are due to the fact that the latter used a cruder model of the nucleus and a considerably simplified approach to description of inelastic collisions of cascade particles. (All of these differences are discussed in detail in our reports<sup>[35, 36]</sup>.)

In the case of low-energy (evaporative) particles, appreciable discrepancies with the theory are observed for the most part only for the softest part of the energy spectrum: for neutrons in the region  $\mathcal{E} < 2$  MeV and for charged particles for  $\mathcal{E} \approx V_{\text{Coul}}$ , where  $V_{\text{Coul}}$  is the effective Coulomb barrier (see Figs. 16 and 17).

In order to obtain an idea of the possible causes of these discrepancies, we will estimate the average lifetime of excited nuclei formed after completion of the

TABLE II. Distribution of number of gray tracks  $n_g$  (in %) in photoemulsion stars containing protons with energies above 30 and 100 MeV (primary-proton energy  $T = 385$  MeV)

$n_g$	$\mathcal{E} > 30$ MeV		$\mathcal{E} > 100$ MeV	
	Theory	Experiment <sup>47</sup>	Theory	Experiment <sup>47</sup>
0	31±5	35±3	60±4	57±4
1	56±6	54±4	34±3	40±4
2	10±1	9±2	6±1	2.5±1
3	2.5±1.0	1.7±0.7	0	—
4	0.5±0.3	—	0	—

TABLE III. Distribution of the fraction of photoemulsion stars containing protons with energies above 30 and 100 MeV, as a function of the number of gray tracks (in %) (primary-proton energy  $T = 385$  MeV)

$n_b$	$\mathcal{E} > 30$ MeV		$\mathcal{E} > 100$ MeV	
	Theory	Experiment <sup>47</sup>	Theory	Experiment <sup>47</sup>
0	98±6	—	82±7	—
1	86±5	81±13	62±6	68±12
2	80±5	77±13	49±3	49±8
3	71±4	66±12	41±3	40±8
4	80±6	61±12	40±5	24±7
5	40±6	52±12	12±8	19±7
6	45±8	23±2	0	12±7
7	0	7±7	0	0

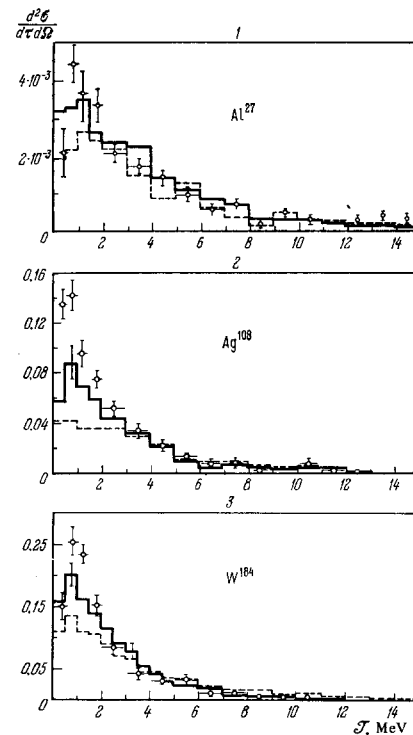


FIG. 17. Energy spectra of evaporation neutrons (in units of  $b/\text{MeV}\cdot\text{sr}$ ) emitted at an angle  $\theta = 180^\circ$  from aluminum, silver, and tungsten bombarded by 150-MeV protons. All of the designations are the same as in Fig. 16.

cascade stage of the interaction. For  $T \approx 150\text{--}200$  MeV in the medium mass-number region ( $A \approx 100$ ) the average excitation energy is  $E^* \approx 50$  MeV (Fig. 18). Then the lifetime of the residual nucleus up to its decay is of the order

$$\tau_{\text{evap}} \sim 1/w_n \sim (30 - 50) \tau_{\text{casc}},$$

where  $w_n$  is the probability of neutron emission calculated from the formulas of statistical evaporation

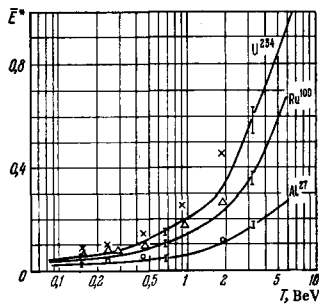


FIG. 18. Average excitation energy (in BeV) of nuclei produced after the end of an intranuclear cascade [38] initiated by a proton with energy  $T$  in nuclei of uranium, ruthenium, and aluminum. The statistical errors of the calculation are shown. The circles, triangles, and crosses show the results of similar calculations by Metropolis et al. [12]

theory<sup>[35]</sup>, and  $\tau_{\text{casc}}$  is the time characterizing the duration of the cascade stage of the interaction and defined as the time of flight of the primary particle over a distance of the order of the nuclear dimensions.

We see that the lifetime of excited nuclei is comparable with the relaxation time of such systems  $\tau_{\text{rel}}$ , which can be roughly estimated as  $\tau_{\text{rel}} \approx (5-10)\tau_{\text{casc}}$ .<sup>[50]</sup>

We recall that we are discussing here only the average excitation energy, whereas the distribution  $W(E^*)$  contains an appreciable fraction of nuclei with greater excitations, up to values  $E^* \approx T$ , corresponding to  $\tau_{\text{evap}} \lesssim 10\tau_{\text{casc}}$ . Thus, even at energies  $T \approx 150-200$  MeV emission of particles can and must occur from excited residual nuclei in which statistical equilibrium has not yet been established, and for energies  $T$  corresponding to an average excitation energy  $E^* \approx 200$  MeV, the separation of the interaction into cascade and evaporative stages itself becomes quite arbitrary.

Up to the present time not a single calculation has been made of the emission of particles from a nonequilibrium excited nucleus produced as the result of a collision with a high-energy particle, but nevertheless we can qualitatively represent the effect of nonequilibrium particle emission by use of the model proposed earlier by Griffin<sup>[51]</sup> and Blann<sup>[52]</sup> for the energy region of several tens of MeV.

By taking into account two-particle residual interactions, Griffin and Blann could describe by the same means the emission of particles both in the statistical-equilibrium stage (ordinary evaporation theory) and in the process of its establishment—in the pre-equilibrium stage. It turned out that particles emitted in the pre-equilibrium stage contribute to various regions of the spectrum  $W(\mathcal{E})$ , depending on the extent to which the nucleus is excited (in terms of the Griffin-Blann model, depending on the number of excitons<sup>[51,52]</sup>). For small excitations where the number of excitons is still small, particle emission is possible with high energies  $\mathcal{E}$ , which qualitatively permits explanation of the high-energy tail in the secondary-particle spectra for primary proton energies  $T$  of several tens of MeV. Many exciton excitations lead with a high probability to emission of low-energy particles in the pre-equilibrium state. Since the excitations of nuclei remaining after passage of the intranuclear cascade, as a rule, have just this nature, we can conclude that nonequilibrium emission of particles must lead to an appreciable softening of the spectra and, at least qualitatively, can ex-

plain the discrepancies noted above between the experimental and theoretical spectra of low-energy neutrons and protons.

As a result of the above it will be particularly interesting to have rather accurate measurements of the spectra of low-energy neutrons and charged particles both at lower energies ( $T \approx 100$  MeV) and higher energies than have been studied up to the present time. In particular, in the transition to the higher-energy region we should expect an increase in the differences between the theoretical and observed quantities<sup>[8]</sup>.

We would also like to remark that in study of stationary and nonstationary decays of highly excited nuclei it is more convenient to utilize reactions with heavy ions than to discuss proton-nuclear and meson-nuclear collisions. A different fraction of the primary-particle energy is carried away by cascade particles in these collisions, as a result of which we always deal in experiments with a wide spectrum of excitation energies in which the high excitations correspond only to the tail of the distribution. In reactions with heavy ions at energies  $T \approx 5-10$  MeV/nucleon where an excited compound system is formed as a result of the collision, the excitation energy  $E^*$  is known rather accurately. In addition, rather high values of  $E^*$  can be obtained in reactions with heavy ions.

For this reason reactions with heavy ions are convenient for study of the competition of fission and evaporation in excited nuclei<sup>[9]</sup>.

The good agreement of the cascade-evaporative model with experiment in the energy region from several tens of MeV to several BeV has permitted construction of an atlas of the main characteristics of inelastic interactions of  $\pi$  mesons and nucleons with nuclei—the multiplicities of secondary particles of various types, their angular and energy distributions, the excitation-energy values, the average angular momenta of the residual nuclei, their distributions in mass number and charge number, and so forth. These data have been obtained for various targets and primary-particle energies and are suitable material for interpolation of intermediate values<sup>[35,38]</sup>. Debugged programs exist for calculation of the more detailed characteristics.

It is necessary to dwell especially on calculation of inelastic interactions of fast particles with light nuclei of the carbon type. To be able to calculate such interactions is very important, in particular, for estimation of the doses received by biological objects in radiation fields. In order to bring the theoretical results on interactions with light nuclei together with experiment, it turns out to be necessary to take into account  $\alpha$  clusters; calculation of the decay of a strongly excited residual nucleus in this case can be carried out by calculation of the corresponding phase space. The results of the calculations are found to be extremely close to the experimental data (see Fig. 13). Here it turns out to be very important to take into account a certain threshold—the minimum excitation energy below which the residual nucleus cannot break up; this substantially increases the fraction of residual nuclei with mass numbers close to the mass number of the target-nucleus<sup>[34]</sup>.

Calculations<sup>[53]</sup> have shown that long-range  $\alpha$  particles with energies above several tens of MeV are particularly sensitive to the  $\alpha$ -cluster structure of

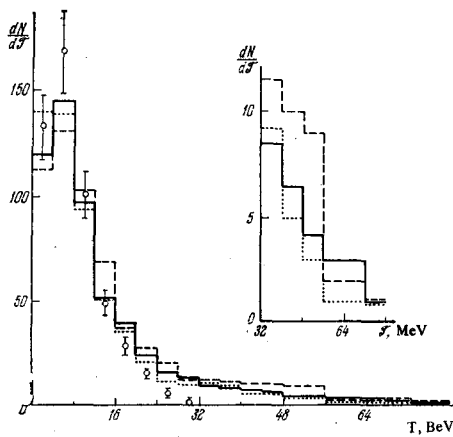


FIG. 19. Energy spectrum of  $\alpha$  particles emitted from  $C^{12}$  nuclei bombarded by 660-MeV protons. The solid, dashed, and dotted histograms are the theoretical results respectively for variants A, B, and C listed in Table IV; the experimental points have been taken from ref. 54.

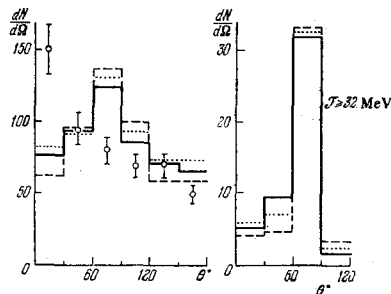


FIG. 20. Angular distribution of  $\alpha$  particles emitted from  $C^{12}$  nuclei bombarded by 660-MeV protons. All of the designations are the same as in Fig. 19. The angular distribution of  $\alpha$  particles with energies  $\mathcal{E} > 32$  MeV is shown separately.

TABLE IV. Number of  $\alpha$  clusters in a spherical layer with radii  $r_1-r_2$  ( $n_\alpha$  is the number of cascade  $\alpha$  particles emitted from the nucleus;  $n_\alpha^{\text{exp}} = 0.15 \pm 0.02$ ; [54]) in parentheses are shown the total numbers of cascade and decay  $\alpha$  particles;  $\sigma_{\text{in}}$  is the cross section for inelastic interactions  $p + C^{12}$ ;  $\sigma_{\text{in}}^{\text{exp}} = 227 \pm 12$  mb [55])

$r_1-r_2, 10^{13}$ cm	Variant of theory		
	A	B	C
0-1.14	0.1	0.1	0.1
1.14-2.93	0.1	0.2	0.2
2.93-4.53	0.83	0.56	0.28
$n_\alpha$	0.16 (0.53)	0.17 (0.54)	0.11 (0.49)
$\sigma_{\text{in}}, \text{mb}$	210	223	230

light nuclei. If clusters are not taken into account, it is generally not possible to explain in terms of the cascade model the large number of these energetic  $\alpha$  particles observed experimentally. For example, in inelastic interactions of 660-MeV protons with carbon nuclei, about one fourth of all secondary  $\alpha$  particles have energies  $\mathcal{E} \geq 32$  MeV, [54] while the ordinary cascade model not taking into account clusters predicts a fraction of such particles  $\approx 3\%$ . [34, 53]

The best agreement with experiment (Figs. 19 and 20 and Table IV) is obtained by assuming that the  $\alpha$  clusters are distributed preferentially at the periphery of the nucleus and their number  $N_\alpha$  in a nucleus is approximately 0.7-0.8, which corresponds to a probability of coagulation of nucleons into  $\alpha$  clusters  $W_\alpha$

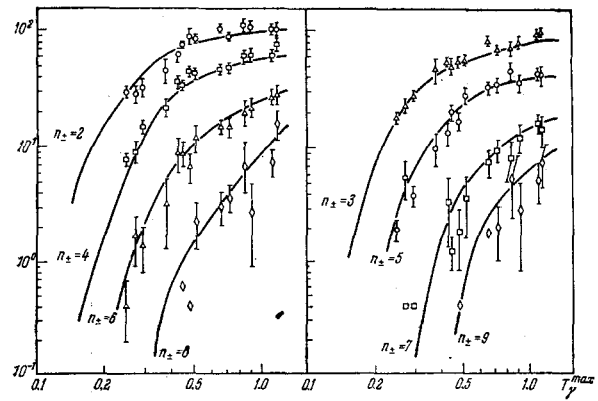


FIG. 21. Yield of stars with number of charged particles  $n_\pm$  in photo-emulsion bombarded by bremsstrahlung photons with maximum energy  $T_{\text{max}}$ . Curves—theoretical result for  $Ti^{50}$ ; the experimental points have been taken from ref. 44.

$\sim 4 N_\alpha / 12 \approx 20-25\%$ . It can be seen from Fig. 9 that after separation of the long-range  $\alpha$  particles, the distribution of the remaining particles with energies  $\mathcal{E} < 32$  MeV is a weak function of the cluster structure of the target-nucleus.

Long-range  $\alpha$  particles are emitted mainly in the large-angle region,  $\theta \sim 80^\circ$  (see Fig. 20). The discrepancy between theory and experiment here can evidently be explained by the fact that at small angles the experimental values of  $dN/d\Omega$  receive an important contribution from  $He^3$  nuclei which have not been separated experimentally. It would be interesting to have a more careful study of the properties of the long-range  $\alpha$  particles, and in particular a measurement of their spectra at different angles.

The cascade-evaporative model is also very effective for calculation of interactions of  $\gamma$  rays with nuclei in the energy region above the giant resonance [56]. In this region the interaction of a  $\gamma$  ray with the intranuclear nucleons leads to formation of two or three fast particles as the result of meson photoproduction or absorption of the  $\gamma$  ray by a quasideuteron pair of nucleons [10]. The relative probability of these processes and the mean free path of the  $\gamma$  ray in the nucleus can be determined by means of the experimental cross sections. Here, as in the case of  $\pi N$  and  $NN$  collisions, in order to reproduce the elementary  $\gamma N$  interaction event inside the nucleus it is convenient to use polynomial approximations of the corresponding experimental distributions (tables of coefficients of these approximations have been given by Il'inov [57]).

It should be noted that in experiments with photonuclear reactions, as a rule, we are dealing with  $\gamma$  rays distributed over the very wide bremsstrahlung spectrum. This somewhat complicates the calculation, but as the result of the further averaging it reduces the requirements on the accuracy of the data used for the elementary  $\gamma N$ ,  $\pi N$ , and  $NN$  interactions. The good agreement of the theoretical calculations with experiment is illustrated in Figs. 14, 21, and 22.

## 6. THE INTRANUCLEAR CASCADE MODEL IN THE ENERGY REGION ABOVE SEVERAL BeV

In the region  $T \approx 3-5$  BeV the cascade model discussed above reveals noticeable discrepancies with experiment which increase rapidly with increasing  $T$ .

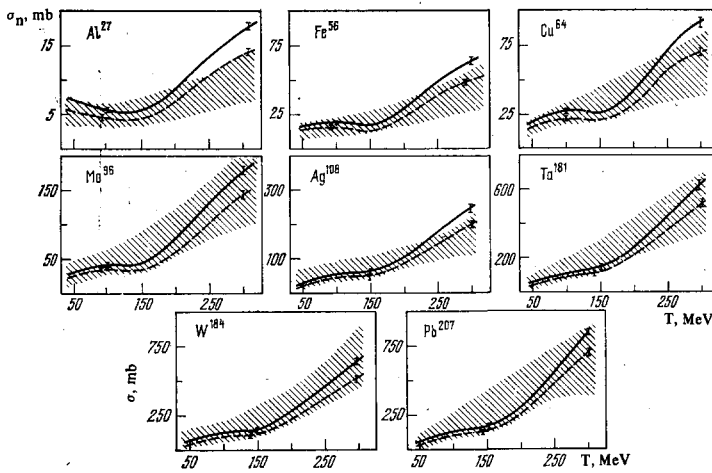


FIG. 22. Cross section for photoproduction of neutrons with energy  $T < 15$  MeV in various nuclei. The shaded regions show the uncertainty in the experiment [58]. The solid and dashed curves are calculations with level-density parameters respectively  $a = A/10$  and  $A/20$ .

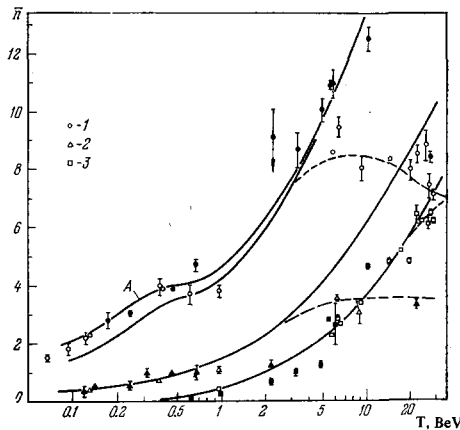


FIG. 23. Average number of s, g, and h particles in photoemulsion stars as a function of primary-proton energy  $T$ . Solid curves—theory; curve A—calculation of  $\bar{n}_h(T)$  for stars with  $n_h > 1$ . The dashed lines show curves which approximate the most reliable experimental points. The symbols marked 1–3 respectively show experimental values of  $\bar{n}_h$ ,  $\bar{n}_g$ , and  $\bar{n}_s$  obtained by along-the-track scanning; the solid symbols refer to values obtained by area scanning of the emulsion.

These discrepancies appear first of all in the characteristics of the low-energy particles produced. For example, from Fig. 23 it is evident that the theoretical values of the average multiplicity  $\bar{n}_g$  and  $\bar{n}_h$  in proton-nuclear collisions are in good agreement with experiment for  $T \lesssim 3-5$  BeV but do not reflect the experimentally observed saturation at higher energies. The theoretical values of  $\bar{n}_s$  are very close to the experimental values up to  $T \approx 20$  BeV, where appreciable discrepancies also begin to appear.

Similar results have been obtained also for pion-nuclear interactions [59].

The difference between the theoretical and experimental characteristics appears more visibly if we consider the correlation of particles. From Fig. 24 we can see that for  $T \lesssim 3-5$  BeV the dependence of  $\bar{n}_g$  on the number of h tracks in a star is in good agreement with experiment, while at higher energies the theoretical histograms differ noticeably from the measured values.

In regard to the dependence of the average number of gray tracks on the number of s particles, for  $T > 3-5$  BeV we cannot consider that there is even qualitative agreement with experiment (Fig. 25). At lower energies there are no direct measurements, but

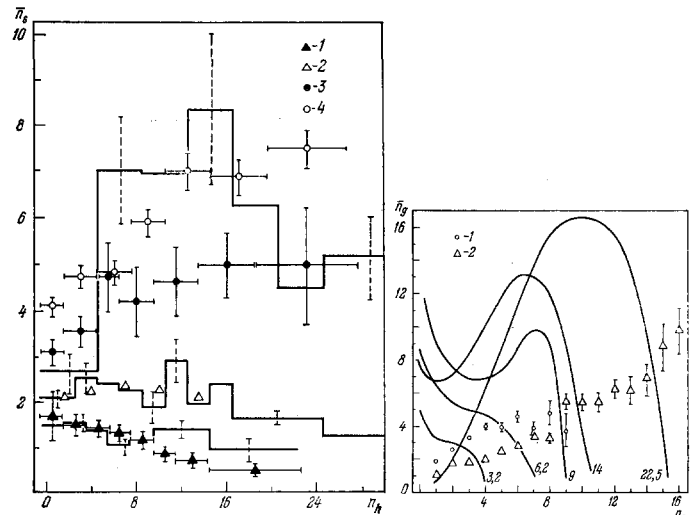


FIG. 24

FIG. 24. Correlation of the average number of s tracks and the number of h tracks in photoemulsion stars produced by  $\pi$  mesons. The symbols marked 1–4 show experimental data respectively for  $T = 1.87, 4.2, 10,$  and  $16.1$  BeV; the histograms show the theoretical calculation for  $T = 1.87, 4.2,$  and  $16.1$  BeV.

FIG. 25. Average multiplicity of g tracks as a function of the number of s particles in photoemulsion stars produced by protons. Curves—theory; the numbers on the curves indicate the primary-proton energy in BeV. 1 and 2 are the experimental data of Winzeler [60] respectively for  $T = 6.2$  and  $22.5$  BeV.

the nature of the correlations for  $T = 3.2$  BeV in proton-nuclear interactions will be roughly the same as in collisions of  $\pi$  mesons with nuclei at  $T = 1.87$  BeV, where a decrease in the average number of g tracks with increasing  $n_s$  is observed. [61]

We can indicate several causes of the discrepancies between the cascade calculations and experiment at energies above several BeV. First of all we must have in mind that all calculations made up to the present time have completely ignored the fact that, as the cascade develops, a larger and larger number of intranuclear nucleons are drawn into it, as a result of which the low-energy component of the cascade particles encounters in its path a smaller density of nuclear matter. Here there is a corresponding reduction also in the excitation energy of the residual nucleus and consequently in the number of evaporative particles.

In order to take into account this fact (it could be

called sweeping the nucleus), we must consider the nucleus not as a continuous distribution of the intranuclear material but as consisting of individual nucleons whose locations must be chosen by the Monte Carlo method according to the appropriate density distribution  $\rho(r)$  obtained in electron-scattering experiments. In distribution of the nucleons the condition is imposed that the distance between their centers not be less than  $2r_c$ , where  $r_c = 0.4 \times 10^{-13}$  cm is the radius of the nucleon core. The coordinates of all intranuclear nucleons are stored in the memory<sup>[62, 63]</sup>.

A fast particle (the primary particle or a particle produced in the course of the intranuclear cascade) can interact with any intranuclear nucleon which turns out to be inside a cylinder with radius  $r_{int} + \lambda$  and axis along the velocity vector of the particle (here  $r_{int}$  is a quantity close to the strong interaction radius and  $\lambda$  is the DeBroglie wavelength of the fast particle considered).

The probability of interaction with the  $i$ -th intranuclear nucleon is determined by the binomial distribution

$$w_i = q^{i-1} (1 - q),$$

where  $q$  is the average probability that the particle will not interact with a nucleon.

In order to evaluate this probability, we note that in the ordinary cascade model with a continuous distribution of nuclear matter the random selection of the interaction point is based on the Poisson distribution for the mean free paths. In this case the probability that a particle with a cross section  $\sigma_t$  experiences  $k$  collisions in a path  $l$  in matter with density  $\rho$  is

$$w(k) = e^{-\rho\sigma_t l} (\rho\sigma_t l)^k / k!.$$

If in a length  $l$  there are  $n$  individual interaction centers and the probability of collision with each of them is  $p$ , then the corresponding Poisson distribution for the probability of experiencing  $k$  collisions in a segment  $l$  has the form

$$w(k, \lambda) = e^{-\lambda} \lambda^k / k!,$$

where  $\lambda = np$ .

In passage of a particle through a nucleus where the number of interaction centers is small, the probability distribution will be binomial for the corresponding Bernoulli series of trials with probability of success  $p$  and of failure  $q$ :

$$w(k, n, p) = [n! / k! (n - k)!] p^k q^{n-k}.$$

This distribution goes over to the usual Poisson distribution  $w(k)$  as  $n \rightarrow \infty$ ,  $p \rightarrow 0$ , and  $\lambda = np = \text{const}$ .

When  $n$  is sufficiently large, the distributions  $w(k)$  and  $w(k, \lambda)$  should agree; in this case

$$\lambda = \rho\sigma_t l$$

and from the expression for  $w(k, \lambda)$  it follows that

$$p = \rho\sigma_t / n.$$

If we take into account further that  $n = \rho\pi(r_{int} + \lambda)^2 l$ , we finally obtain

$$p = 1 - q = \sigma_t / \pi (r_{int} + \lambda)^2.$$

The value of  $p$  can also be determined in another way. From the Poisson distribution  $w(k)$  it follows that the probability that a particle not experience collisions in a segment  $l$  is

$$w(0) = e^{-\rho\sigma_t l}.$$

The same probability obtained from the distribution  $w(k, n, p)$  is

$$w(0, n, p) = (1 - p)^n = q^n.$$

If we assume that  $w(0) = w(0, n, p)$ , then

$$q = \exp(-\rho\sigma_t l / n) = \exp[-\sigma_t / \pi (r_{int} + \lambda)^2].$$

For  $\sigma_t / \pi (r_{int} + \lambda)^2 \ll 1$  the two approaches obviously give the same result.

An important detail of the model being considered is the fact that the nuclear nucleon with which the interaction occurred is from then on considered a cascade particle and not a component part of the nuclear system; a consequence of this is the change in the nuclear density on passage of a cascade avalanche.

In regard to the elementary  $\pi N$  or  $NN$  interaction event, its calculation is carried out by exactly the same means as described above.

In modeling the fate of cascade particles in the nucleus, it is necessary first of all to follow the most energetic particle. This permits the development of the intranuclear cascade in time to be approximately taken into account.

In Fig. 26 we have shown the energy dependence of the multiplicity of avalanche particles and slow particles, calculated with inclusion of the decrease in density of intranuclear nucleons. We see that in this case the necessary effect is actually achieved. It is important that at the lower energies the theoretical results practically coincide with the data obtained on the basis of the ordinary cascade model<sup>[62, 63]</sup>. The same can be said also of the theoretical values of the particle correlations (Figs. 27 and 28).

The theoretical quantities in Figs. 22–24 were obtained for a parameter value  $r_{int} = 1.3 \times 10^{-13}$  cm. Variation of  $r_{int}$  by as much as 20–30%, although it affects the absolute values of the secondary-particle multiplicity, does not change the general nature of the theoretical curves. The results of the calculations are still less sensitive to the choice of  $r_c$ .

It is important to emphasize that the theoretical results turn out to be extremely sensitive to the conditions for selection of events in regard to the value of  $n_h$ . In photoemulsion experiments this point is very delicate: separation of interactions with hydrogen of the photoemulsion is carried out, as a rule, on the basis of the criterion  $n_h > 1$ , but here it is possible to lose a significant fraction of the interactions with nuclei, and this in turn can very substantially affect the values of  $\bar{n}_s$  and  $\bar{n}_h$ .

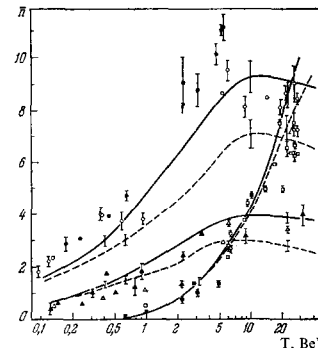


FIG. 26. Energy dependence of the average multiplicity of  $s$ ,  $g$ , and  $h$  particles, calculated with inclusion of the change in density of intranuclear nucleons. The dashed lines show the results of calculations made with the condition  $n_h > 1$ ; all remaining designations are the same as in Fig. 23.

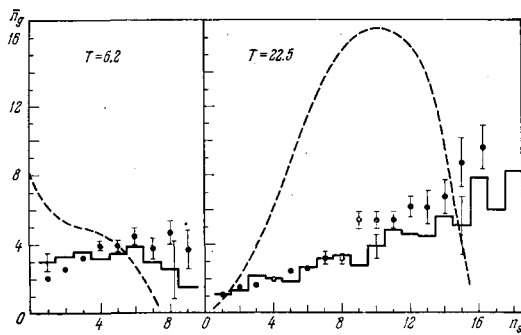


FIG. 27. The same as Fig. 25 (solid histograms—theory with inclusion of the change in density of intranuclear nucleons).

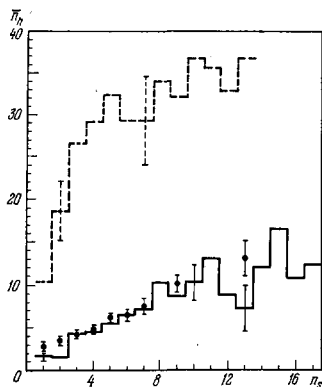


FIG. 28. Average multiplicity of  $h$  particles as a function of the number of thin tracks in a photoemulsion star produced by a  $\pi$  meson with energy  $T = 17.2$  BeV. All the designations are the same as in Fig. 27; the experimental points have been taken from ref. 64.

It is interesting that in the ordinary cascade-evaporative model, which gives a monotonic rise of  $\bar{n}_g(T)$  and  $\bar{n}_h(T)$ , the role of the selection criteria decreases with increasing energy  $T$ , and in the region  $T > 1$  BeV they can be completely neglected<sup>[14]</sup>.

The energy value  $T$  at which the multiplicity  $\bar{n}_g(T)$  and  $\bar{n}_h(T)$  reaches a plateau (or reaches some maximum; see Fig. 26) depends on the type of target-nucleus. In particular, for light nuclei of the  $C^{12}$  type saturation is reached already at  $T \approx 0.5-1$  BeV<sup>[11]</sup>.

The decrease in density of intranuclear matter with development of the cascade leads to a saturation of the number of recoil nucleons and of the excitation energy of the residual nucleus. This permits the qualitative explanation of a number of important facts related to the phenomena of fragmentation and fission of nuclei. Thus, if we assume that fragments are nucleon clusters knocked out of a nucleus by cascade nucleons or formed as the result of evaporation from the excited residual nucleus, then the rise of the cross sections for their production should slow at energies  $T$  of the order of several BeV, which actually is observed experimentally. Furthermore, since the main part of the mass lost by the target-nucleus occurs to  $h$  particles, the parameters characterizing the mass distribution of the residual nuclei as a function of energy  $T$  also should reach a saturation in the energy region of the order of several BeV. Analysis of radiochemical measurements for nuclei in the middle of the periodic table confirms this conclusion.

In the energy region above several hundred MeV, with further increase of the primary-proton energy the rise in excitation energy only partially compensates the increase of the fission barrier produced by deeper and deeper disintegration of the nuclei. This leads to a decrease in the fission cross section  $\sigma_f$  with increasing

$T$ . However, at energies of the order of several BeV and above, this decrease should slow down. The conclusion also is confirmed by the results of recent measurements<sup>[65,66]</sup>. None of the effects which have just been enumerated is explained by the ordinary cascade model.

In addition to the change in density of intranuclear nucleons, there is an additional effect which is not usually taken into account in cascade calculations and which in principle can provide an appreciable contribution for  $T > 1$  BeV. This effect is that, for energies above several BeV in  $\pi N$  and  $NN$  collisions, resonances begin to be intensely produced which, if their lifetime is sufficiently great, can then be drawn into the intranuclear cascade. Actually, for resonances with widths  $\Gamma \sim 100-200$  MeV the lifetime in their proper coordinate system is  $\sim (0.7-0.3) \times 10^{-23}$  sec. If we now take into account the relativistic time dilation and the Pauli principle (the latter is important for low-energy isobars), this time is quite sufficient for a resonance, before it decays, to be able to interact with a nuclear nucleon. From the kinematic point of view this is equivalent to several adhering particles interacting with an intranuclear nucleon at the same time. Here the effective number of intranuclear collisions should decrease, and this will entail a decrease in the excitation energy of the nucleus and in the number of slow particles, which consist mainly of recoil nucleons.

Il'inov and Toneev<sup>[67]</sup> have evaluated the effect of resonance production on those secondary-particle characteristics in which an appreciable deviation is observed from the predictions of the ordinary cascade-evaporative model at high energies. The calculations were made by the Monte-Carlo method in such a way that, with reasonable assumptions as to the interaction cross sections and other properties of the resonances, their contribution was greatest. Since the information on the cross sections for production of resonances and even more so on their interaction with nucleons is very scarce, following assumptions were made regarding the production and subsequent fate of resonances in the nucleus:

a) The production cross sections have been most completely measured for the  $\rho$  and  $\omega$  mesons and the  $\Delta(1236)$  isobar (see the compilation by Behrend et al.<sup>[68]</sup> and the references cited there). An analysis shows that the relative contribution of resonance channels to reactions with three or four particles in the final state is particularly large in the energy region from the reaction threshold up to values as high as  $T \approx 1-2$  BeV, reaching  $\approx 80-100\%$ . With further increase of energy the fraction of events with resonance production drops, and at energies  $T \approx 10$  BeV amounts to about  $10-60\%$ , depending on the type of reaction. For collisions with a large number of particles in the final state and for the production cross sections of other resonances, the corresponding information is quite fragmentary. However, the existing data indicate that in the energy region  $T < 30$  BeV the probability of simultaneous production of two or more resonances is comparatively small. Thus, a reasonable estimate of the probability of resonance production is the assumption that one resonance is produced in each inelastic collision.

b) The kinematic characteristics of resonances have been modeled by combining two particles produced in an elementary inelastic interaction:

$$P_{\text{res}} = P_1 + P_2, \quad E_{\text{res}} = E_1 + E_2,$$

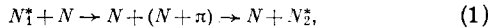
where  $p_i$  and  $E_i$  are the momentum and energy of the  $i$ -th secondary particle; here the resonance mass is defined by the relation  $M_{\text{res}} = (E_{\text{res}}^2 - p_{\text{res}}^2)^{1/2}$ . In spite of a certain arbitrariness in this procedure, it retains the previous correct multiplicity and appearance of the angular and energy distributions of the secondary particles in each elementary event (after breakup of the resonance). In addition, the use of experimental data to find values of  $p_i$  permits us to hope that some anomalies contained in the experimental distributions will be reproduced, which should be reflected also in the mass spectrum  $M_{\text{res}}$ . The latter circumstance is evidently most important for the three-particle channel, whose characteristics have been specially singled out in this discussion<sup>[19]</sup>.

By joining various pairs of secondary particles we can obtain both meson and baryon resonances. For simplicity we will take into account only baryon resonances, which combine a nucleon and a  $\pi$  meson.

c) Information on the interaction of unstable particles with nucleons is practically nonexistent<sup>[20]</sup>. Therefore it was assumed that the characteristics of interaction of a resonance with a particle are the same as for a NN collision (or a  $\pi$ N interaction in the case of a meson resonance) for the same center-of-mass energy of the colliding particles. This refers to the interaction cross sections, to all the characteristics of elastic and inelastic collisions, and also to the potential for interaction of the resonance with the nucleus.

d) The lifetime of the resonance produced was always assumed sufficiently large that the probability of its decay inside the nucleus could be neglected.

These assumptions (which we will call below the main variant or variant I), being likely, are in many respects determined also by the purpose formulated above for the investigation. This follows directly from points a) and d). In addition, in this model a new process appears—the process of resonance survival:



which also acts to increase the effect of resonance production on the global characteristics of the nuclear reaction.

Figure 29 shows the calculated average multiplicity of s, g, and h particles produced by a high-energy proton in a collision with a photoemulsion nucleus. Also shown for comparison are the results of calculations with the ordinary cascade model not taking into account resonance production. As can be seen, the two calculations turn out to give rather similar results and do not reflect the experimentally observed saturation in aver-

age multiplicity  $\bar{n}_h(T)$  and  $\bar{n}_g(T)$  at energies above 3–5 BeV. The difference between these models becomes more noticeable if we consider the average number of intranuclear collisions  $\bar{n}_{\text{coll}}$  (Table V). For an energy  $T = 20$  BeV, inclusion of resonance production leads to a decrease of about 20% in  $\bar{n}_{\text{coll}}$ . For comparison we should recall that inclusion of the decrease in the density of nuclear matter in development of the intranuclear cascade in this energy region gives values of  $\bar{n}_{\text{coll}}$  smaller by a factor of ten.

In order to clarify the sensitivity of the result obtained to inaccuracies in the parameters characterizing the process with participation of resonances, we carried out an additional series of calculations.

There are definite experimental indications that meson resonances are produced preferentially in  $\pi$ N collisions, and baryon resonances in interaction of two nucleons. This fact is taken into account in the second variant of the calculation (see Table V). It must be emphasized that as a consequence of the large difference in the cross sections for  $\pi$ N and NN interactions (particularly in the energy region  $T \lesssim 5$  BeV) the cross section for the resonance-particles interaction also changes considerably. We can expect that the effect of resonances will appear even more strongly if we place in correspondence with the interaction of a resonance with a particle the data for  $\pi$ N and NN collisions not for the same total energy in the center-of-mass system but for the same relative energy (variant III). As can be seen from Table V, the value of  $\bar{n}_{\text{coll}}$  in the two cases actually drops somewhat in comparison with the main variant, but this is far from sufficient to explain the experimentally observed effect.

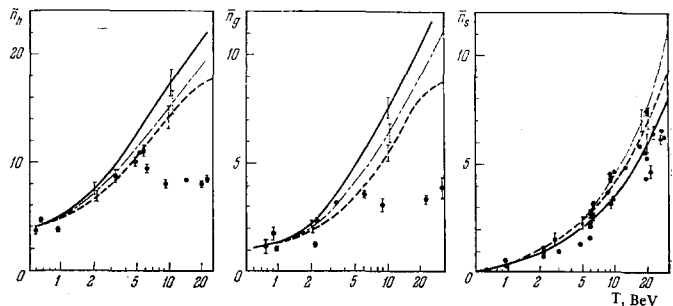


FIG. 29. Energy dependence of the average multiplicity of s, g, and h particles produced by protons interacting with photoemulsion nuclei. The solid, dot-dash, and dashed curves refer respectively to calculations with the ordinary cascade model and to the variants in which one and two resonances, respectively, are produced in each inelastic collision (see the details in ref. 67); the experimental points are the same as in Fig. 23.

TABLE V. Average number of intranuclear collisions in interactions with a  $\text{Ga}^{70}$  nucleus of protons with energy  $T$  (the assumptions made in each variant of the theory are explained in the text; the errors shown are purely statistical)

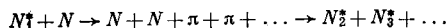
Interaction	T, BeV						
	0,6	1	2	5	10	20	30
Ordinary cascade model		7.95±0.46	12.1±0.7	23.7±1.4	38.1±2.6	59.2±4.4	80.0±4.6
I	4.85±0.30	5.68±0.33	8.35±0.50	17.6±1.1	31.4±2.4	48.0±3.6	
II			8.70±0.49	17.5±1.2	24.9±1.9	40.6±0.3	
III	4.58±0.27	5.88±0.34	7.30±0.44	16.7±1.0	29.2±2.0	42.6±3.3	
IV	4.84±0.29	6.15±0.36	9.40±0.54	16.3±1.0	29.1±2.2	49.1±3.6	
V			8.5±0.5	20.0±1.2	29.7±1.7	49.0±3.7	72.0±5.7
VI		5.44±0.32	7.90±0.46	14.4±0.8	23.2±1.5	39.0±3.0	43.5±3.2

Collisions of baryon resonances with intranuclear nucleons lead to appearance of a new  $\pi$ -meson absorption process<sup>[71]</sup>:



This possibility is taken into account in variant IV, where it is assumed that reaction (2) occurs instead of the quasi-two-particle reaction (1), and the remaining assumptions are exactly the same as in the main variant. The role of the new  $\pi$ -meson absorption mechanism is extraordinarily strengthened in variant V, where in addition to the conditions of calculation of the third-variant it was assumed that instead of the elastic scattering of resonances a reaction described by Eq. (2) occurs. However, even at the price of these assumptions it has not been possible to achieve any improvement of the results.

Finally, assumption a) was strengthened, it being assumed that inelastic collisions with production of four or five secondary particles proceed always with production of two resonances (variant VI). This leads not only to survival of the resonances but also to their multiplication:



However, even for such an extremely exaggerated estimate, the number of collisions  $\bar{n}_{\text{coll}}$  for  $T \approx 30$  BeV decreases only by a factor of two, which is completely insufficient to explain the experimentally observed saturation of  $\bar{n}_g(T)$  and  $\bar{n}_h(T)$  (see Fig. 29).

All of the variants considered also do not explain the behavior of the correlations of the average multiplicity of  $g$  particles with the number of relativistic tracks in the star, and this characteristic is most sensitive to the nuclear-reaction mechanism. Thus, the observed discrepancy in the theoretical and experimental data in the region  $T > 3-5$  BeV is due mainly to the decrease in the number density of intranuclear nucleons and not to the contribution of resonances. This conclusion can be qualitatively explained from the following simple considerations. The decrease in the average multiplicity of secondary particles will be more significant, the greater the number of cascade particles which have been combined into resonances. However, considering the magnitude of the average energies of the particles, it is easy to be convinced that up to  $T \sim 20$  BeV only particles of the first and second generations take a principal part in resonance formation, and their fraction in relation to the total number of particles in the cascade avalanche is comparatively small.

It must of course be kept in mind that we are discussing here only the main characteristics of the interaction; for the individual reaction channels it is clearly possible to point out quantities which will depend substantially on resonance production. However, this is a special problem.

From the kinematic point of view, absorption of a resonance by intranuclear nucleons is to a certain degree equivalent to the process in which several adhering mesons interact at once with a nucleon, which in the very high energy region effectively takes into account the many-particle interaction mechanism which we now proceed to discuss.

In conclusion of this section we will dwell briefly on the sensational results of Marinov et al.<sup>[72]</sup> on the pos-

sibility of nucleon-nuclear processes with anomalously large momentum transfer to the target-nucleus.

In this work a tungsten target was bombarded for a long time by 24-BeV protons, after which a chemical separation was made of the fractions of various elements, and a spontaneously fissile emitter was observed in the mercury fraction. Since mercury does not undergo spontaneous fission, the observed radiation was assigned to the chemical analog of mercury—the element with charge  $Z = 112$ , which could be formed in fission of a superheavy nucleus obtained as the result of fusion of two tungsten nuclei: the target-nucleus and the recoil nucleus. For such a fusion to occur, the energy of the recoil nucleus must exceed the Coulomb barrier of the reaction  $V_{\text{Coul}} \approx 1$  BeV. According to the estimates of Marinov et al.<sup>[72]</sup>, in order to explain the observed yield of the spontaneously fissile emitter, the cross section for production of tungsten nuclei with energy  $\mathcal{E} > 1$  BeV must be about  $10^{-30}$  cm<sup>2</sup>.

In order to check this conclusion, experiments were carried out on the direct detection of recoil nuclei with charge  $Z \gtrsim 15-20$  and with kinetic energy  $\mathcal{E} > 4-6$  MeV/nucleon in bombardment of Ta nuclei by high-energy neutrons in the 76-BeV accelerator at Serpukhov<sup>[73]</sup> and in bombardment of W, Au, and U nuclei by 24-BeV protons in the 32-BeV accelerator at Brookhaven<sup>[74]</sup>. These experiments gave an upper limit for the combined cross section for production of such nuclei  $(2-6) \times 10^{-33}$  cm<sup>2</sup>, which is 200-500 times smaller than the value determined by Marinov et al.<sup>[72]</sup> On the basis of these data the conclusion of Marinov et al.<sup>[72]</sup> on their observation of an element with  $Z = 112$  and correspondingly the conclusion of existence of some processes with anomalously high momentum transfer to the target-nucleus are at least debatable.

## 7. INTRANUCLEAR CASCADES AT ULTRAHIGH ENERGIES $T \gg 10$ BeV

In the transition to the very high energy region the emission angles of particles produced in  $\pi N$  and  $NN$  collisions, as a consequence of the relativistic contraction, become so small that any discrimination in the times of interaction of these particles with an intranuclear nucleon becomes meaningless; in other words, in this case simultaneous scattering and absorption occur of several particles by one nucleon (Fig. 30)<sup>[16,17]</sup>. Here the avalanche of fast particles turns out to be localized along a comparatively narrow channel, and therefore the effect of sweeping the nucleus can be neglected in the first approximation.

Since we know practically nothing at the present time about the properties of many-particle interactions, it is expedient to consider the inverse problem—to attempt to obtain information on these interactions from analysis of experimental data obtained in cosmic-ray experiments. The calculation must begin, of course, with the most general assumptions as to the nature of many-particle interactions and introduce details only as this becomes absolutely necessary to reconcile the theoretical and experimental results. This will serve as a

FIG. 30. At the point A an ordinary two-particle inelastic interaction occurred; at point B a many-particle interaction occurred.

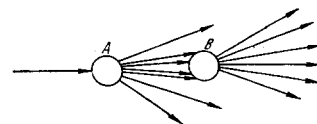


TABLE VI. Comparison with experiment of cascade-theory result taking into account many-particle interactions

T, BeV	Interaction	Characteristic	Theory	Experiment*
100	p + LEm	$\bar{n}_s$	7.9±0.4	7.4±0.5
		$\bar{\mathcal{E}}_s$ , BeV	3.1±0.2	2.9±0.3
	p + Fm	$\bar{n}_s$	10.3±0.5	8.0±0.5
		$\bar{n}_g$	3.6±0.2	5.0±1.6
200	$\pi^-$ + LEm	$\bar{n}_s$	2.8±0.2	2.4±0.9
		$\theta_{(1/2)s}^0$	9.7±0.4	8.0±0.9
	$\pi^-$ + Em	$\bar{n}_s$	6.5±0.3	6.2±0.4
		$\theta_{(1/2)s}^0$	11.2±0.6	10.8±0.9
	$\pi^-$ + HEm	$\bar{n}_s$	9.0±0.5	8.3±0.6
		$\theta_{(1/2)s}^0$	14.7±0.7	14.7±2.0
500	p + Em	$\bar{n}_s$	12.0±0.6	11.0±1.1
		$\bar{n}_g$	18.0±0.9	18.8±4.2
10 <sup>3</sup>	p + LEm	$\bar{n}_s$	3.7±0.2	4.0±0.8
		$\bar{n}_g$	12.1±0.6	9.9±1.4
	p + Em	$\bar{n}_s$	20.5±1.1	22.5±3.0
		$\bar{n}_g$	3.6±0.2	4±1.6

\*See the bibliography in ref. 17. LEm, Em, and HEm are medium-light, medium, and medium-heavy photoemulsion nuclei;  $\bar{\mathcal{E}}_s$  is the average energy of the secondary particles (after subtraction of the leading particle);  $\theta_{(1/2)s}^0$  is the angle into which half of the s particles are emitted (in the laboratory system).

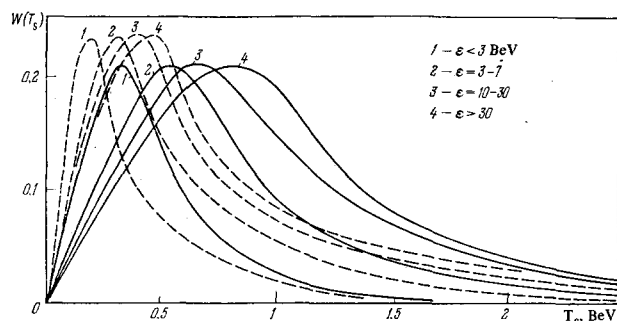


FIG. 31. Energy distributions of pions (dashed lines) and heavy particles (solid lines) produced in inelastic many-particle interactions. Center-of-mass system;  $\epsilon = [(\sum E_i)^2 - (\sum p_i)^2]^{1/2} - \sum M_i$  is the free energy which can be expended in formation of new particles ( $E_i$ ,  $M_i$ ,  $p_i$  are the energies, masses, and momenta of the particles).

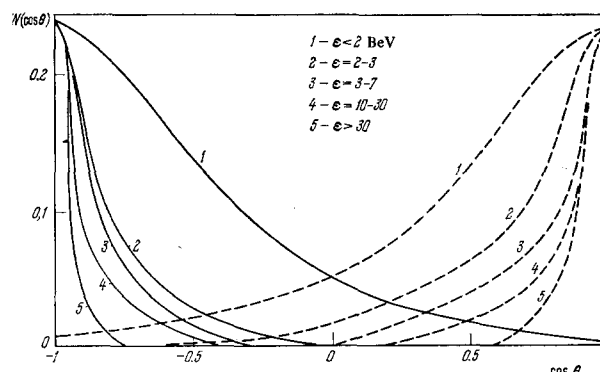


FIG. 32. Angular distributions of pions and heavy particles produced in inelastic many-particle interactions (CMS, the designations are the same as in Fig. 31).

definite protection from introduction of unjustified assumptions.

The calculations have shown that in this case it is possible to obtain a number of well defined and quite general conclusions<sup>[17]</sup>. In particular, we can consider reliably established the very existence of many-particle interactions and the fact that the characteristics of particles produced in such interactions are close to those observed in ordinary two-particle interactions at high energies, for example, the existence of a leading particle and the asymmetric nature of the angular distributions of the remaining particles (Figs. 31 and 32). Table VI and Fig. 33 illustrate how well the theoretical values taking into account many-particle interactions agree with experiment.

In the energy region of the order several hundred BeV the number of many-particle interactions amounts to several tens of percent of the number of all intranuclear collisions<sup>[17]</sup>. At energies of the order of several tens of BeV the situation is more complex, since here it is necessary, simultaneously with the many-particle interactions, to take into account the effect of sweeping the nuclei. Calculations in which both these effects are taken into account have not yet been carried

out. The size of the contribution of many-particle interactions in the region  $T \approx 10-100$  BeV requires clarification. We see that in the energy region  $T \gg 1$  BeV many aspects of the intranuclear-cascade mechanism remain unclear. In particular, experiments in the 70-BeV accelerator at Serpukhov and proposed measurements at  $T \approx 500$  BeV in the Batavia accelerator can substantially clear up the picture of many-particle interactions—of this important new type of elementary-particle interaction.

It should also be noted that at very high energies the theoretical results obtained by means of stationary evaporation theory agree with experiment significantly more poorly than in the region  $T \lesssim 1$  BeV. For example, the average number of low-energy particles and their energy turn out to be substantially higher than the experimental values<sup>[17]</sup>. The cause of this discrepancy requires clarification.

## 8. THEORY OF INELASTIC COLLISIONS OF TWO NUCLEI

A significant part of the information on strong interactions in the ultrahigh-energy region is presently obtained from analysis of inelastic collisions of nuclei,

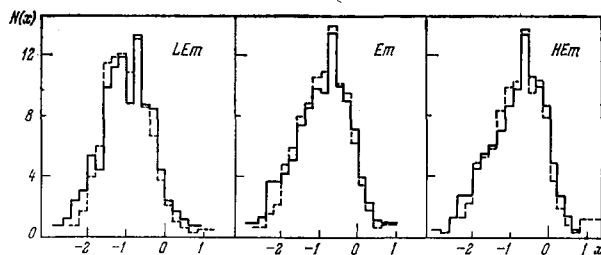


FIG. 33. Distribution of thin tracks in photoemulsion stars produced by  $\pi$  mesons with energy  $T \approx 200$  MeV, as a function of the quantity  $x = \log \tan \theta$ . Solid histograms—experimental data [75], dashed curves—theoretical result. LEm and HEm—interaction with light and heavy photoemulsion nuclei, Em—interaction calculated for the average photoemulsion nucleus.

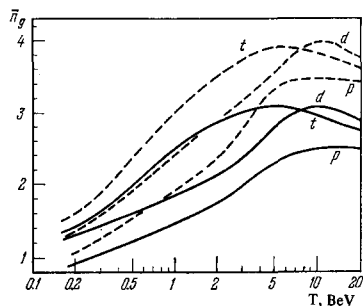


FIG. 34. Energy dependence of the average multiplicity of gray tracks produced in inelastic collisions of protons, deuterons, and tritium nuclei with photoemulsion nuclei. The solid curves are for all inelastic interactions, and the dashed curves are for events with  $n_h > 1$ .

and therefore the study of the mechanism of such collisions is an extremely pressing problem. To learn how to calculate processes occurring in nuclear collisions with energy greater than several hundred MeV per nucleon is extremely important also in connection with calculations of radiation shielding and the design of high-current accelerators. At the present time such calculations are hindered both by severe mathematical difficulties and by the unclear nature of the physical picture of the process. It still remains unclear how to take into account the change in the properties of the target-nucleus as it is filled by nucleons of the incident nucleus; it is also unclear what is the contribution of interference of cascades produced by different nucleons of the incident nucleus, and a number of other questions.

At the present time the interactions are calculated successfully only with the very simplest nuclei: deuterons, tritium, and  $\text{He}^3$  and  $\text{He}^4$  nuclei. Intranuclear cascades in these cases are the sum of the cascades produced in the target-nucleus by the individual nucleons of the incident nucleus. In the high-energy region it turns out to be essential to take into account the reduction in density of the target-nucleus as the result of ejection of the nucleons composing it, as we should expect, this effect appears at lower energies for nucleus + nucleus interactions and for collisions of pions and nucleons with nuclei. For example, for tritium + nucleus collisions this effect must be taken into account already at  $T \approx 1$  BeV/nucleon (Fig. 34).

In the case of deuteron-nucleus interactions it turns out to be important in description of the differential cross sections in the small-angle region to take into account also peripheral diffraction disintegrations of the deuteron. How important this process and also Coulomb disintegration are for heavier nuclei is still

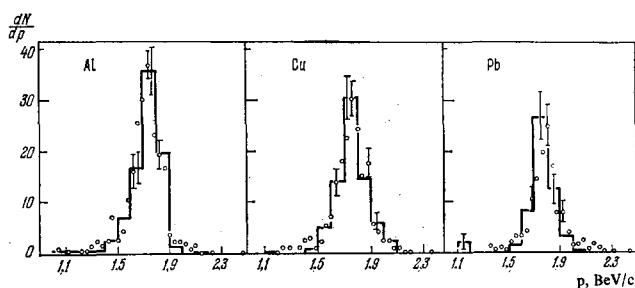


FIG. 35. Momentum distributions of protons produced in inelastic collisions of deuterons with nuclei at  $T = 1.05$  BeV/nucleon. Histograms—theoretical result; the experimental points have been taken from ref. 79.

TABLE VII. Cross sections for inelastic deuteron-nuclear interactions at energies  $T = 80$  MeV/nucleon (in barns)

Target	Theory	Experiment <sup>76</sup>
Al <sup>27</sup>	1.16 ± 0.06	0.966 ± 0.05
Cu <sup>64</sup>	1.99 ± 0.07	1.76 ± 0.17
Ta <sup>181</sup>	3.68 ± 0.20	3.13 ± 0.30
Pb <sup>207</sup>	3.72 ± 0.18	3.44 ± 0.17
U <sup>238</sup>	4.05 ± 0.14	3.81 ± 0.15

unclear, primarily because of the absence of experimental data with which the theoretical results could be compared.

The decay of the excited residual nuclei, as in the case of interactions of particles with nuclei, is calculated by means of evaporation theory. In spite of discrepancies with experiment in individual details, the cause of which remains unclear (it is not excluded that this is due to a significant degree also to experimental errors), the results obtained by means of the cascade-evaporative model on the whole satisfactorily reproduce the known experimental data. How good the agreement is can be seen from Tables VII and VIII and Figs. 35–37 and 39. More detailed data are given in the literature<sup>[83]</sup>.

In regard to heavier incident nuclei, this is still terra incognita. Experiments in this direction can provide extremely interesting results which also have a definite practical value. For example, in processes with large momentum transfer in collisions of nuclei there is the possibility in principle of obtaining secondary mesons with an energy which significantly exceeds the nominal energy of the accelerator. This follows from the scale invariance of strong interactions recently formulated by Balzin<sup>[84]</sup>. The spectra of high-energy secondary particles produced in the collision of relativistic nuclei are determined mainly by the local properties of hadronic matter, and the geometrical characteristics of the colliding objects play a secondary role in this case<sup>[84]</sup>. We can expect that these spectra and the spectra of particles from “elementary”  $\pi N$  and  $NN$  interactions will be described by the same universal function  $f(p_2/p_1)$ , where  $p_1$  is the incident-nucleus momentum and  $p_2$  is the secondary-particle momentum. If the interaction of nuclei with large momentum transfer is discussed here as the result of a many-particle interaction, the absolute value of the cross section for production of secondary particles with anomalously high energies will be determined by the probability of incidence of nucleons in the many-particle interaction region:

$$P_N = 1 - (1 - A^{-N})^{A/NI} (A-N)!$$

TABLE VIII. Distribution in number of prongs  $W(n)$  (in %) of photoemulsion stars produced by deuterons with energy  $T$ .

$n$	$T = 110 \text{ MeV/nucleon}$		$T = 137 \text{ MeV/nucleon}$	
	Theory *)	Experiment <sup>77</sup>	Theory	Experiment <sup>78</sup>
0	$5.0 \pm 0.5$	—	$7.4 \pm 0.6$	$23.5 \pm 5.3$
1	$21.0 \pm 1.1$	$12.8 \pm 0.9$	$17.0 \pm 1.0$	$21.2 \pm 5.0$
2	$26.5 \pm 1.8$	$33.2 \pm 1.5$	$23.4 \pm 1.1$	$22.4 \pm 5.1$
3	$22.2 \pm 1.1$	$22.0 \pm 1.2$	$18.0 \pm 1.0$	$16.5 \pm 4.4$
4	$15.9 \pm 1.0$	$16.5 \pm 1.0$	$15.5 \pm 0.9$	$9.4 \pm 3.3$
5	$8.5 \pm 0.6$	$10.5 \pm 0.8$	$11.0 \pm 0.7$	$4.7 \pm 2.3$
6	$3.7 \pm 0.4$	$3.0 \pm 0.5$	$5.2 \pm 0.4$	$2.3 \pm 1.6$
7	$1.5 \pm 0.2$	$2.0 \pm 0.4$	$1.6 \pm 0.2$	0
8	$0.7 \pm 0.1$	0	$0.6 \pm 0.1$	0
9	—	—	$0.3 \pm 0.1$	0

\*) Since events in which only neutral stars are produced were not considered in ref. 77, the theoretical distribution  $W(n)$  has been normalized to the total number of stars with  $n > 0$ .

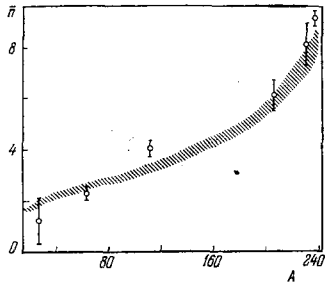


FIG. 36. Average number of neutrons produced in an inelastic deuteron-nucleus interaction at  $T = 80 \text{ MeV/nucleon}$ . The shaded region corresponds to the uncertainty in calculation of evaporation neutrons; the experimental points have been taken from ref. 80.

We see that the probability of participation in a many-particle collision of all nucleons of a nucleus with large mass number  $A$  is negligible, but this probability becomes quite significant for comparatively large groups of nucleons. This opens the possibility in principle of increasing the energy of particles in presently existing accelerators at the price of a definite reduction in intensity.

The hypothesis of scale invariance has found recent confirmation in an experiment on observation of high-energy pions produced in collisions of relativistic deuterons with nuclei (Fig. 38).

## 9. CONCLUSION

We see that the intranuclear cascade model permits agreement with experiment to be attained over the entire energy region from several tens of MeV to several BeV, and when the change in density of intranuclear matter and many-particle interactions are taken into account—also at significantly higher energies. At the same time, a number of questions requiring further solution are associated with this model.

It is more difficult to obtain agreement for low-energy (evaporation) secondary particles for the same set of parameters, independent of the primary-particle energy. Development of the nonstationary theory of particle emission from highly excited nuclei is required for this purpose.

For the further refinement of the cascade-evaporative model, it is of interest to study not so much the integrated average characteristics as the differential distributions and the correlations between individual quantities. The low-energy component of the particles produced deserves special attention.

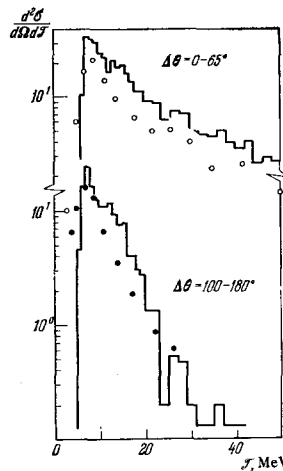


FIG. 37

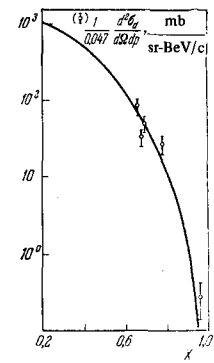


FIG. 38

FIG. 37. Energy spectra of protons (in  $\text{mb/sr-MeV}$ ) emitted in the angular interval  $\Delta\theta$  in interaction of 205-MeV  $\alpha$  particles with silver nuclei. Histogram—theoretical result; the experimental points have been taken from ref. 81.

FIG. 38. Comparison of experimental data on the cross section for production of pions by deuterons with the theoretical function describing the cross section for production of pions by protons.  $X$ —ratio of momentum of the pion produced to the maximum possible momentum in the reactions  $d + N \rightarrow \pi + \dots$  and  $p + N \rightarrow \pi + \dots$  [85]

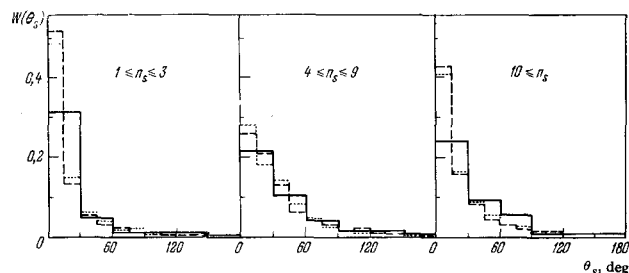


FIG. 39. Angular distributions of cascade particles in stars with various numbers of  $s$  tracks, produced in inelastic collisions of cosmic-ray  $\alpha$  particles ( $T > 600 \text{ MeV}$ ) with photoemulsion nuclei. Solid histogram—experimental data from ref. 82; theoretical curves are shown for two forms of the cosmic-ray energy distribution:  $W(T) \sim (1+T)^{-2.9}$  (dashed line) and  $W(T) \sim (1+T)^{-2.5}$  (dotted histogram).

Only the first steps have been taken in creation of a theory of inelastic collisions of high-energy particles. Substantial work is required also to explain the phenomena of fragmentation and emission of fast deuterium, tritium, and helium nuclei. In this field theory is still a long way behind experiment.

- <sup>1</sup>A beam of relativistic deuterons with energy about 5 BeV/nucleon has been available at Dubna since 1970.
- <sup>2</sup>The review is an expanded version of lectures given at the School of High Energy Physics held at Varna in June, 1971, jointly by JINR and CERN.
- <sup>3</sup>We designate by T everywhere the kinetic energies of the primary particles in the laboratory system and the corresponding secondary-particle energies.
- <sup>4</sup>The nucleus is considered to be a degenerate Fermi gas of nucleons enclosed in the nuclear volume. According to the Pauli principle the nucleons, after an intranuclear collision, must have energies above the Fermi energy; otherwise such an interaction is forbidden. The action of the Pauli principle leads in effect to an increase of the mean free path of fast particles inside the nucleus.
- <sup>5</sup>We must note the success of the approximation based on the model of N\* resonance decay. As the calculations of Bertini [<sup>18</sup>] have shown, in spite of its obvious crudeness this approach gives quite good numerical results up to energies  $T \approx 3$  BeV; this method turns out to be extremely simple in its calculational aspect.
- <sup>6</sup>In calculations in the very high energy region above several tens of BeV, it is necessary to take into account individually by means of the inelasticity coefficient K the contribution of the so-called leading particle, which in the laboratory system carries away on the average about 60% of the primary-particle energy. The experimental distributions of the inelasticity coefficient are also satisfactorily reproduced by means of polynomial approximations. The energy dependence of the quantities  $a_N$ ,  $b_N$ , and  $p_{\max}$  in the region  $T \gg 10$  BeV turns out to be smoother and can be approximated by logarithmic terms of the type  $\sum_{k=0}^M b_{nk} (\ln T)^k$  (more detail on this question can be found in our report [<sup>22</sup>]).
- <sup>7</sup>The important difference between these calculations and those carried out in all earlier studies lies first of all in the substantially more accurate modeling of  $\pi N$  and NN collisions inside the nucleus. Diffuseness of the nuclear boundary and of the nuclear potential were taken into account in the cascade calculations (the nuclear-density parameters were taken from experiments on electron scattering); it was taken into account that inside the nucleus a potential  $V_\pi$  different from zero acts on a  $\pi$  meson as on a nucleon; the possibility of absorption of a slow  $\pi$  meson by bound nucleons of the nucleus was taken into account. The decay of the excited residual nucleus was calculated by the Monte-Carlo method according to evaporation theory.
- <sup>8</sup>From the theoretical point of view the study of neutron spectra is preferable to study of charged-particle spectra, since in this case there is no uncertainty due to the poor knowledge of the Coulomb-barrier height.
- <sup>9</sup>We will not discuss here the fission of excited residual nuclei, since the theory of this phenomenon has not yet been well developed at the present time and the theoretical results have essentially a semi-quantitative and sometimes even simply qualitative nature.
- <sup>10</sup>The Compton effect in an intranuclear nucleon can be neglected, since its cross section is small in comparison with the cross sections of other processes.
- <sup>11</sup>Calculations show that the "sweeping" of the nuclei affects the energy and angular characteristics of the particles produced significantly more weakly [<sup>14</sup>]. This also explains the rather good agreement with experiment of the calculations carried out previously with the ordinary cascade model.
- <sup>12</sup>In experiments on photoproduction of mesons from nuclei, estimates have been obtained of the cross sections for interaction of  $\rho$  and  $\omega$  mesons with nucleons. According to the data of recent studies  $\sigma_{\rho N} \approx \sigma_{\omega N} \approx \sigma_{\pi N}$ . [<sup>68-70</sup>].
- <sup>1</sup> V. G. Bobkov, V. P. Demin, I. B. Keirim-Markus, E. E. Kovalev, A. V. Larichev, V. A. Sakovich, L. N. Smirennyĭ, and M. A. Sychkov, Radiatsionnaya bezopasnost' pri kosmicheskikh poletakh (Radiation Safety in Space Flight), Moscow, Atomizdat, 1964.
- <sup>2</sup> O. D. Brill', A. I. Vikhrov, S. S. Gorodkov, F. P. Denisov, V. E. Dudkin, E. E. Kovalev, O. V. Lozhkin, V. I. Ostroumov, and L. N. Smirennyĭ, Yadernye vzaimodeĭstviya v zashchite kosmicheskikh korablĕi (Nuclear Interactions in Space-Ship Shields), Moscow, Atomizdat, 1968.
- <sup>3</sup> The AECL Study for an Intense Neutron Generator, ed. by C. A. Bartholomew and P. R. Tunnicliffe Rept. AECL-2600, Chalk River, 1966.
- <sup>4</sup> Discussion on the Electronuclear Method of Obtaining Energy, Atomnaya ėnergiya 29, 151, 158, 162 (1970).
- <sup>5</sup> A. M. Baldin, Report JINR R7-5808, Dubna, 1971.
- <sup>6</sup> D. I. Blokhintsev, V. S. Barashenkov, and B. M. Barbashov, Usp. Fiz. Nauk 68, 417 (1959) [Sov. Phys.-Uspekhi 2, 505 (1960)].
- <sup>7</sup> P. E. Hodgson, The Optical Model of Elastic Scattering, Oxford, Clarendon Press, 1963. Russ. transl., Atomizdat, 1966, chapter 3.
- <sup>8</sup> R. J. Glauber, in Lectures in Theoretical Physics, vol. 1, ed. by W. E. Brittin and L. G. Dunham, N. Y.-L., Interscience, 1959.
- <sup>9</sup> V. S. Barashenkov and V. D. Toneev, Usp. Fiz. Nauk 100, 425 (1970) [Sov. Phys. Uspekhi 13, 182 (1970)].
- <sup>10</sup> W. Czyż and L. C. Maximon, Ann. Phys. (N.Y.) 52, 59 (1969).
- <sup>11</sup> M. L. Goldberger, Phys. Rev. 74, 1268 (1948).
- <sup>12</sup> N. Metropolis, R. Bivins, M. Storm, J. H. Miller, and G. Friedlander, Phys. Rev. 110, 185 (1958).
- <sup>13</sup> V. S. Barashenkov, V. M. Maltsev, and E. K. Mihul, Nucl. Phys. 24, 642 (1961).
- <sup>14</sup> V. S. Barashenkov, K. K. Gudima, and V. D. Toneev, Acta Phys. Polon. 36, 457, 887 (1969).
- <sup>15</sup> V. S. Barashenkov, K. K. Gudima, and V. D. Toneev, Yad. Fiz. 10, 755 (1969) [Sov. J. Nucl. Phys. 10, 436 (1970)].
- <sup>16</sup> I. Z. Artykov, V. S. Barashenkov, and S. M. Eliseev, Nucl. Phys. 87, 83, 241 (1966).
- <sup>17</sup> I. Z. Artykov, V. S. Barashenkov, and S. M. Eliseev, Nucl. Phys. B6, 11 (1968); I. Z. Artykov and V. S. Barashenkov, Nucl. Phys. B6, 628 (1968).
- <sup>18</sup> H. W. Bertini, Phys. Rev. 188, 1711 (1969).
- <sup>19</sup> V. S. Barashenkov, K. K. Gudima, and V. D. Toneev, Reports JINR R2-4065 and R2-4066, Dubna, 1968; Acta Phys. Polon. 36, 415 (1969).
- <sup>20</sup> E. Byckling and K. Kajantie, Nucl. Phys. B9, 568 (1969).
- <sup>21</sup> G. I. Kopylov, Zh. Eksp. Teor. Fiz. 35, 1426 (1958); 39, 1091 (1960) [Sov. Phys. JETP 8, 996 (1959); 12, 761 (1961)].
- <sup>22</sup> V. S. Barashenkov and S. M. Eliseev, Report JINR R2-5331, Dubna, 1970.
- <sup>23</sup> B. Baldoni, S. Focardi, H. Hromadnic, L. Monari, F. Saporetti, S. Femino, F. Mezzanares, E. Bertolini, and G. Gialanella, Nuovo Cimento 26, 1376 (1962); W. J. Fickinger, E. Pickup, D. K. Robinson, and E. O. Salant, Phys. Rev. 125, 2082 (1962).
- <sup>24</sup> T. Vishki, I. M. Gramenitskiĭ, Z. Korbil, A. A. Nomo-filov, M. I. Podgoretskiĭ, L. Rob, V. N. Strel'tsov, D. Tuvdendorzh, and M. S. Khvastunov, Zh. Eksp. Teor. Fiz. 41, 1069 (1961) [Sov. Phys. JETP 14, 763 (1962)].
- <sup>25</sup> M. Dsejthey-Barth, Nuovo Cimento 32, 545 (1964).
- <sup>26</sup> Y. Baudinet-Robinet, M. Morand, Tsai Chü, C. Castagnoli, G. Dascola, S. Mora, A. Barbaro-Galtieri, G. Baroni, and A. Manfredini, Nucl. Phys. 32, 452 (1962).
- <sup>27</sup> N. A. Dobrotin, V. V. Guseva, K. A. Kotelnikov, A. M. Lebedev, S. V. Ryabikov, S. A. Slavatinsky, and N. G. Zelevinskaya, Nucl. Phys. 35, 152 (1962).
- <sup>28</sup> A. A. Kamal and G. K. Rao, Nucl. Phys. B2, 135 (1967).
- <sup>29</sup> E. Lohrmann, Nuovo Cimento 5, 1074 (1957);

- S. Kapeko, O. Kusumoto, S. Matsumoto, and M. Takahata, Trudy Mezhdunarodnoi konferentsii po kosmicheskim lucham (Proceedings Intern. Conf. on Cosmic Rays), Vol. 1, Moscow, Nauka, 1960; M. W. Teucher, D. M. Haskin, and M. Schein, Phys. Rev. 111, 1384 (1958); L. Montanet, J. A. Newth, G. Petrucci, R. A. Salmeron, and A. Zichichi, Nuovo Cimento 17, 166 (1960); M. Schein, D. M. Haskin, E. Lohrmann, and M. W. Teucher, Phys. Rev. 116, 1238 (1959); S. Matsumoto, J. Phys. Soc. Japan 18, 1 (1963).
- <sup>30</sup> V. V. Guseva, N. A. Dobroton, N. G. Zelevinskaya, K. A. Kotelnikov, A. M. Lebedev, and S. A. Slavatskiy, J. Phys. Soc. Japan 17, Suppl. A-III (1962).
- <sup>31</sup> I. Z. Artykov, V. S. Barashenkov, and S. M. Eliseev, Yad. Fiz. 4, 156 (1966) [Sov. J. Nucl. Phys. 4, 113 (1967)].
- <sup>32</sup> N. M. Sobolevskii and V. D. Toneev, Acta Phys. Polon. 35, 367 (1969).
- <sup>33</sup> K. J. LeCouteur, in Yadernye reaktsii (Nuclear Reactions), Vol. 1, Moscow, Gosatomizdat, 1962; I. Dostrovsky, P. Rabinowitz, and R. Bivins, Phys. Rev. 111, 1659 (1958); I. Dostrovsky, Z. Fraenkel, and G. Friedlander, Phys. Rev. 116, 683 (1959); V. S. Barashenkov, V. M. Mal'tsev, and V. D. Toneev, Izv. AN SSSR, ser. fiz. 30, 322, 337 (1966) [Bull. USSR Acad. Sci., Phys. Ser. 30, 327, 342 (1966)].
- <sup>34</sup> O. B. Abdinov and V. S. Barashenkov, Reports JINR R2-4788, Dubna, 1969; R2-5023 and R4-5479, Dubna, 1970.
- <sup>35</sup> V. S. Barashenkov, A. S. Il'inov, N. M. Sobolevskii, and V. D. Toneev, Report JINR R2-5549, Dubna, 1970.
- <sup>36</sup> H. W. Bertini, Phys. Rev. 131, 1801 (1963); Reports ORNL-3383 1963; ORNL-3787 1966; ORNL-TM-2699 1966.
- <sup>37</sup> V. D. Toneev, JINR Preprint B1-2740, Dubna, 1966.
- <sup>38</sup> V. S. Barashenkov, K. K. Gudima, A. S. Il'inov, and V. D. Toneev, Report JINR R2-5118, Dubna, 1970.
- <sup>39</sup> V. S. Barashenkov, A. S. Il'inov, N. M. Sobolevskii, and V. D. Toneev, Report JINR R2-5507, Dubna, 1970.
- <sup>40</sup> I. Nonaka, Y. Saji, A. Suzuki, H. Yamaguchi, R. Eisberg, Y. Ishisaki, K. Kikuchi, K. Matsuda, T. Mikumo, and Y. Nakajima, J. Phys. Soc. Japan 17, 1817 (1962).
- <sup>41</sup> J. W. Washter, W. A. Gibson, and W. R. Burrus, ORNL-TM-2253, Oak Ridge, 1968.
- <sup>42</sup> V. A. Kon'shin, E. S. Matushevich, and V. I. Regushevskii, Yad. Fiz. 4, 337 (1966) [Sov. J. Nucl. Phys. 4, 242 (1967)].
- <sup>43</sup> R. D. Edge, D. H. Tompkins, and G. W. Glenn, Phys. Rev. 183, 849 (1969).
- <sup>44</sup> C. E. Roos and V. Z. Peterson, Phys. Rev. 124, 1610 (1961).
- <sup>45</sup> M. Bercovitch, H. Carmichael, G. C. Hanna, and E. P. Hincks, Phys. Rev. 119, 412 (1960).
- <sup>46</sup> R. G. Vasil'kov, B. B. Govorkov, V. I. Gol'danskiĭ, V. A. Kon'shin, O. S. Lupandin, E. S. Matushevich, B. A. Pimenov, S. S. Prokhorov, and S. G. Tsypin, Yad. Fiz. 7, 88 (1968) [Sov. J. Nucl. Phys. 7, 64 (1968)].
- <sup>47</sup> G. Bernardini, E. T. Booth, and S. J. Lindenbaum, Phys. Rev. 85, 826 (1952).
- <sup>48</sup> V. S. Barashenkov, V. M. Mal'tsev, and V. D. Toneev, Izv. AN SSSR, ser. fiz. 30, 232 (1966) [Bull. USSR Acad. Sci., Phys. Ser. 30, 237 (1966)].
- <sup>49</sup> N. T. Porile, Phys. Rev. 120, 572 (1960).
- <sup>50</sup> T. Ericson, Adv. Phys. 9, 425 (1960).
- <sup>51</sup> J. J. Griffin, Phys. Rev. Letters 17, 478 (1966).
- <sup>52</sup> M. Blann, Phys. Rev. Letters 21, 1357 (1968).
- <sup>53</sup> O. A. Abdinov and V. S. Barashenkov, Report JINR R2-5939, Dubna, 1971.
- <sup>54</sup> A. P. Zhdanov and P. I. Fedotov, Zh. Eksp. Teor. Fiz. 43, 835 (1962) [Sov. Phys. JETP 16, 590 (1963)].
- <sup>55</sup> V. I. Moskalev and B. V. Gavrilovskii, Dokl. Akad. Nauk SSSR 110, 972 (1956) [Sov. Phys. Doklady 1, 607 (1957)].
- <sup>56</sup> K. K. Gudima, A. S. Il'inov, and V. D. Toneev, JINR Reports R2-4661 and R2-4808, Dubna, 1969.
- <sup>57</sup> A. S. Il'inov, Kand. dissertatsiya (Ph.D. Dissertation), JINR, 1971.
- <sup>58</sup> L. W. Jones and K. M. Terwillinger, Phys. Rev. 91, 699 (1953).
- <sup>59</sup> V. S. Barashenkov, K. K. Gudima, and V. D. Toneev, Yad. Fiz. 10, 755 (1969) [Sov. J. Nucl. Phys. 10, 436 (1970)].
- <sup>60</sup> H. Winzeler, Nucl. Phys. 69, 661 (1965).
- <sup>61</sup> B. E. Ronne and O. Danielsson, Ark. Fys. 22, 175 (1962).
- <sup>62</sup> V. S. Barashenkov, A. S. Il'inov, and V. D. Toneev, JINR Communication E2-5282, Dubna, 1970.
- <sup>63</sup> V. S. Barashenkov, A. S. Il'inov, and V. D. Toneev, Yad. Fiz. 13, 743 (1971) [Sov. J. Nucl. Phys. 13, 422 (1971)].
- <sup>64</sup> J. M. Kohli, Nucl. Phys. B14, 500 (1969).
- <sup>65</sup> E. S. Matushevich and V. N. Regushevskii, Yad. Fiz. 7, 1187 (1968) [Sov. J. Nucl. Phys. 7, 708 (1968)].
- <sup>66</sup> G. Hudis and S. Katcoff, Phys. Rev. 180, 1122 (1969).
- <sup>67</sup> A. S. Il'inov and V. D. Toneev, JINR Report R2-5546, Dubna, 1971.
- <sup>68</sup> H. J. Behrend, F. Lobkowicz, E. H. Thorndike, A. A. Wehmann, and M. E. Nordberg, Jr., Phys. Rev. Letters 24, 1246 (1970).
- <sup>69</sup> H. J. Behrend, F. Lobkowicz, E. H. Thorndike, and A. A. Wehmann, Phys. Rev. Letters 24, 336 (1970).
- <sup>70</sup> H. Alvensleben, U. Becker, W. K. Bertram, M. Chen, K. J. Cohen, T. M. Knasel, R. Marshall, D. J. Quinn, M. Rohde, G. H. Sanders, H. Schubel, and S. C. C. Ting, Phys. Rev. Letters 24, 786 (1970).
- <sup>71</sup> Z. Fraenkel, Phys. Rev. 130, 2407 (1963).
- <sup>72</sup> A. Marinov, C. J. Batty, A. I. Kilvington, G. W. A. Newton, V. J. Robinson, and J. D. Hemingway, Nature 229, 464 (1971).
- <sup>73</sup> G. N. Flerov, Yu. P. Gangrsky, and O. A. Orlova, JINR Communication E7-5887, Dubna, 1971.
- <sup>74</sup> S. Katcoff and M. L. Perlmann, Preprint BNL-15829, Bookhaven, 1971.
- <sup>75</sup> J. Gierula and S. Krzywdzinski, Nuovo Cimento 55A, 370 (1968).
- <sup>76</sup> G. P. Millburn, W. Birnbaum, W. E. Crandall, and L. Schecter, Phys. Rev. 95, 1268 (1954).
- <sup>77</sup> L. P. Solov'eva, Zh. Eksp. Teor. Fiz. 31, 1086 (1956) [Sov. Phys. JETP 4, 923 (1956)].
- <sup>78</sup> M. V. K. Appa Rao and P. J. Lavakare, Nuovo Cimento 29, 321 (1963).
- <sup>79</sup> R. L. Lander, O. Piccioni, Nguyen-hen Xuong, and P. Yager, Phys. Rev. B137, 1228 (1965).
- <sup>80</sup> W. E. Crandall and G. P. Millburn, J. Appl. Phys. 29, 698 (1958).
- <sup>81</sup> L. E. Bailey, UCRL-3334 (Thesis), Berkeley, 1956.
- <sup>82</sup> M. Ceccarelli, G. Quarenzi, and G. T. Zorn, Nuovo Cimento 1, 669 (1955).
- <sup>83</sup> V. S. Barashenkov, K. K. Gudima, and V. D. Toneev, Yad. Fiz. 9, 528; 10, 760 (1969) [Sov. J. Nucl. Phys. 9, 302 (1969); 10, 439 (1970)]; K. K. Gudima, A. D. Kirillov, V. D. Toneev, and Yu. P. Yakovlev, JINR Report R2-5261, Dubna, 1970; V. S. Varashenkov,

A. S. Il'inov, and V. D. Toneev, JINR Report R2-5548, Dubna, 1971; T. A. Gabriel, R. T. Santoro, and R. G. Alsmiller, Jr., Preprint ORNL-TM-3153, Oak Ridge, 1970.

<sup>84</sup>A. M. Baldin, Kr. Soobshch. fiz. (Brief communications in physics), FIAN, SSSR, No. 1, 35 (1971).

<sup>85</sup>A. M. Baldin, T. Giordenescu, V. N. Zubarev, A. D.

Kirillov, V. A. Kuznetsov, N. S. Moroz, V. B. Radomanov, V. N. Ramlin, V. A. Sviridov, V. S. Stavinskiĭ, and M. I. Yatsuta, Preprint JINR R1-5819, Dubna, 1971.

Translated by C. S. Robinson